FINAL ENGINEERING REPORT

DESIGN, DEVELOPMENT, FABRICATION,

AND TEST,

IMPROVED MAGNETIC TAPE RECORDER

JPL SUBCONTRACT 951128

PREPARED FOR:

Jet Propulsion Laboratory
California Institute of Technology
Pasadena, California

JPL SUBCONTRACT 951128

PREPARED BY:

Kinelogic Corporation
29 South Pasadena Avenue
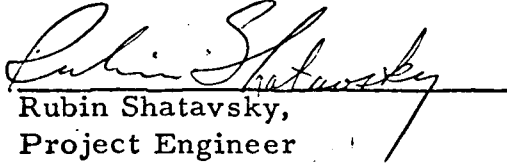Pasadena, California 91101

(213) 684-0434

TWX 919-588-3287

DISTRIBUTION

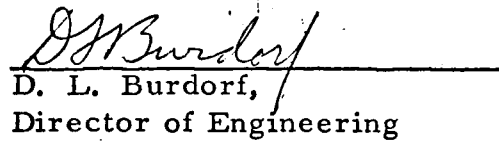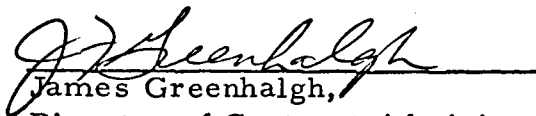| Copy Number	Recipient
1 - 10	Jet Propulsion Laboratory, California Institute of Technology, Pasadena, California
11	R. Shatavsky, Project Manager, Kinelogic Corporation
12	J. Greenhalgh, Director of Contract Administration, Kinelogic Corporation
13	Engineering Files, Kinelogic Corporation
14	Publications Files, Kinelogic Corporation

APPROVALS

Prepared by:

Rubin Shatavsky,
Project Engineer

Approved by:

D. L. Burdorf,
Director of Engineering

Approved by:

James Greenhalgh,
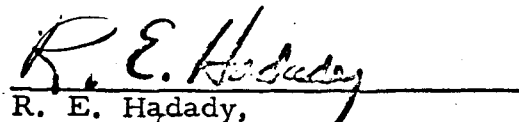Director of Contract Administration

Approved by:

R. E. Hadady,
Director of Marketing

TABLE OF CONTENTS

FINAL ENGINEERING REPORT

DESIGN, DEVELOPMENT, FABRICATION, AND TEST,

ENGINEERING TEST MODEL

IMPROVED MAGNETIC TAPE RECORDER

1.   CONTRACT FULFILLMENT

This final engineering report is submitted in fulfillment of Jet Propulsion

Laboratory subcontract number 951128, Article 2, item (b) (7), by Kinelogic

Corporation.

2.   SUMMARY

During the period beginning 31 December 1964 and ending 17 October 1966,

Kinelogic Corporation has performed work for the Jet Propulsion Laboratory of

the California Institute of Technology in accordance with subcontract 951128,

National Aeronautics and Space Administration contract NAS 7-100.

In accordance with the original subcontract specifications, Kinelogic

Corporation designed an improved magnetic tape recorder in a configuration of

6 x 6 x 2-1/4 inches. In designing in this configuration, several unique

mechanical designs were developed and a study of available bearings was made.

New environmental requirements imposed upon the design dictated that

a redesign be made. The new design required a housing configuration of

6 x 7-3/4 inches. There were new developments in the area of belts and hermetic

sealing of the housing.

An improved magnetic tape recorder designated as the Engineering Test

Model (ETM) was built and tested. The results of the tests indicated that the

design fulfilled the goal parameters for the program.

3. INTRODUCTION

Typically, tape recorders that are to be used for obital or interplanetary missions are required to exhibit small size, low weight low power consumption, and high reliability. These parameters as measured against data capacity are indexes of efficiency for such a device. Work done under JPL contracts 950903, Worst Case Analysis, 950899, Tape Recorder Belt Study and 950795, Tape Guidance Study, indicated that further improvements in tape transport design could be realized. To this end JPL sponsored this subcontract to design, develop and fabricate an Engineering Test Model (ETM) which would take advantage of these studies in the design of an Iso-Elastic reel-to-reel machine.

This report a) explains the Iso-Elastic Drive system in general terms (3. 1) and in specific terms (Appendix A), and b) discusses the program history (3. 2) of the 6 x 6 configuration (3. 2. 1), and the new environmental conditions (3. 2. 2) which occasioned the change to the 6 x 7-3/4 configuration (3. 2. 3).

3.1   TAPE TRANSPORT FUNCTION AND THE ISO-ELASTIC DRIVE

3.1.1   Tape Transport Function

The tape transport is used to move the tape past the record/reproduce

magnetic heads at a constant speed. The tape is under predetermined tension

as it moves across the head area so that proper tape-to-head contact is

achieved. In a conventional reel-to-reel recorder, the supply reel plays the

tape off under a hold-back tension and the take-up reel winds up the tape as

it is paid out of the head area by the constant speed drive mechanism--generally

a rotating capstan and pressure roller combination.

3.1.2   Problems With Conventional Recorder

Varying rotational speeds in reeling systems present a major design

problem in providing constant tension winding with reels whose tape pack

diameters and, hence, moment arms, are constantly changing. It is evident

that angular reel speeds change simultaneously with the build-up and reduction

of tape packs.

Most reel-to-reel tape deck designs use center driven reel hubs. The

basic speed variation problem is usually accommodated through the use of an

overrunning clutch on the lead spool and a drag brake on the following spool.

Individual opposed torque motors on supply and take-up spools are also used.

These methods are wasteful of power and mechanically complex. Other

techniques include differentially coupling supply and take-up reels through

negator springs. This latter approach finds considerable favor in low power

satellite recorders, but requires a separate capstan drive system and also is

rather complicated mechanically.

7

3.1.3   The Iso-Elastic Drive

The ETM developed under JPL subcontract 951128 employs the Kinelogic-originated Iso-Elastic Drive system. The Iso-Elastic Drive is described and analyzed in detail in the technical paper, "New Concept in High Reliability Tape Recorders for Spaceborne Data Storage", by D. L. Burdorf, which is included as Appendix A to this report.

Briefly, the Iso-Elastic Drive system employs a seamless polyester belt riding directly on the outer layer of the tape in each reel, as shown in Figure 1. The belt is driven by two capstans, one of which operates at a speed of 0.35% faster than the other. Because of this differential, a constant predetermined tension is developed dynamically in the tape while between the two reels. Since the tape is moved past the magnetic heads under constant tension, no capstan and capstan pressure idlers are required. The tape moves past the heads at a constant rate, thus minimizing the flutter. Because of its simplicity and because the net power of the two-capstan system approaches zero, the power required for operation of the Iso-Elastic Drive system is very minimal. Furthermore, since this system reduces the number of parts by a considerable percentage, the system weight is effectively reduced.

3.2   PROJECT HISTORY

The technical description of the Improved Magnetic Tape Recorder in the original contract specified a recorder with a 6-inch by 6-inch by 2 1/2-inch or less configuration with no specific reliability requirements. Modification 2 to the subject contract 21 October 1965 established a reliability requirement of a 90% probability of surviving the 4400 hours of continuous operation at 4 ips.
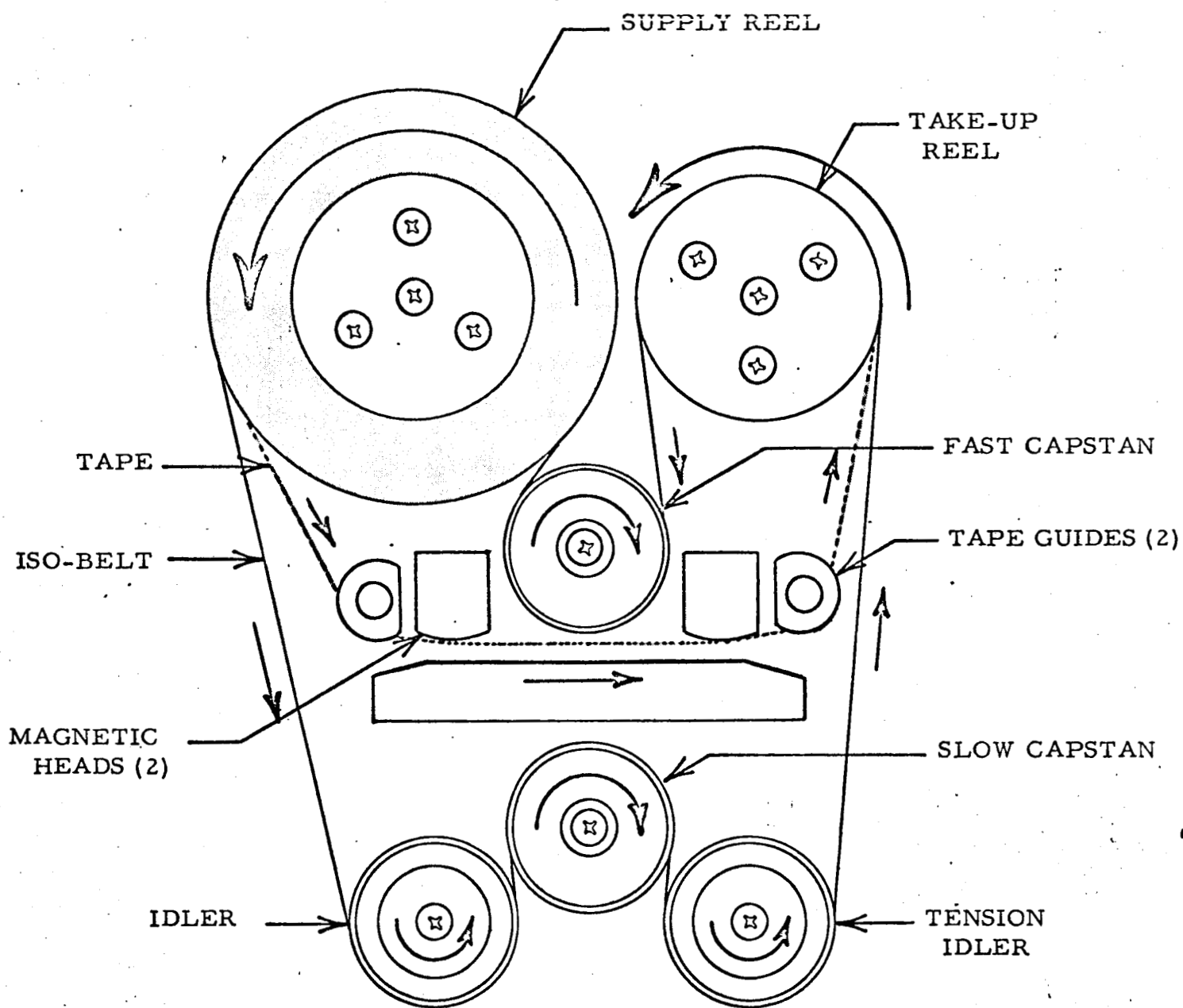
SUPPLY REEL

TAKE-UP REEL

TAPE

ISO-BELT

MAGNETIC HEADS (2)

IDLER

FAST CAPSTAN

TAPE GUIDES (2)

SLOW CAPSTAN

TENSION IDLER

FIGURE 1, ISO-ELASTIC DRIVE SYSTEM, ETM RECORDER

3.2   PROJECT HISTORY (Continued)

The imposition of this reliability requirement precluded the use of the 6 x 6 configuration and resulted in a change to a 6 x 7-3/4 inch configuration. Both configurations are discussed here under separate headings.

3.2.1   6 x 6 Configuration (and related activities)

During the initial phase of the project, a review of the Belt Study* and Worst Case Analysis** was made. During this time, preliminary layout work was progressing. Several meetings were held with the cognizant engineers who had engaged in these studies. Various approaches to bearing applications were considered. Many bearing preloading schemes were considered, and an iso-belt tensioning system was investigated.

3.2.1.1   Belt Application and Preliminary Layout

A review of the Belt Study* program report indicated that greater life can be expected with Kapton (H-film) belts than from Mylar belts. The endurance limit of Kapton belts is 35% greater than that of Mylar. At life below the endurance limit, this figure is exceeded greatly. Therefore, it was decided to proceed using belts of Kapton.

The approach taken in the mechanical design was to select the largest possible capstan and idler diameters to maximize the smallest bend radius of the Iso-Elastic Drive system belt. The motor speed reduction transmission system using seamless polyester belts, was then designed around the

*   Tape Recorder Belt Study, Final Report on Fatigue of Seamless Polyester
     and Polyimide Film Belts.

** Reliability Analysis of Tape Recorder Model ETM

- 6 -

3. 2. 1. 1   Belt Application and Preliminary Layout (Continued)

requirements of the Iso-Elastic Drive system. After considerable design effort,

the configuration shown in Figure 2 was selected. Idlers and capstans of 7/16

inch in diameter were determined to be the maximum diameter compatible within

the 6 x 6 configuration.

3. 2. 1.2   Iso-Belt Tensioning System

An iso-belt tensioning system was designed employing two eccentrically

mounted idlers. Figure 2 shows the location of the tension idlers in the

Iso-Elastic Drive system. Figure 3 shows a section view of the eccentric

tension idler as proposed.

3. 2. 1. 3   Bearing Preloading Schemes

Consideration was given to various bearing preloading schemes. Figure 4

shows the several schemes considered. The system shown in Figure 4 K was

adopted as the preferred scheme because it has taken advantage of being a fixed

system which does not incorporate loose shims that can easily be displaced.

3. 2. 1. 4   Bearing Selection

Various ball bearing manufacturers were contacted in order to gain

information on a quality assurance program on purchased bearings. New

Hampshire Ball Bearing Company proposed the following:

1.   52100 chrome steel - approximately 20% greater

       load carrying capacity than 303 stainless steel, but

       at the risk of possible corrosion of bearings.

2.   One shield and one Teflon seal if the higher torque

       is acceptable.

BEARING
(DUPLEX PAIR)

PRECISION SPACER

IDLER

BEARING
(DUPLEX PAIR)

BASE PLATE

SPRING MOUNT

COUNTER-
BALANCE

NEGATOR SPRING
(HELICAL)
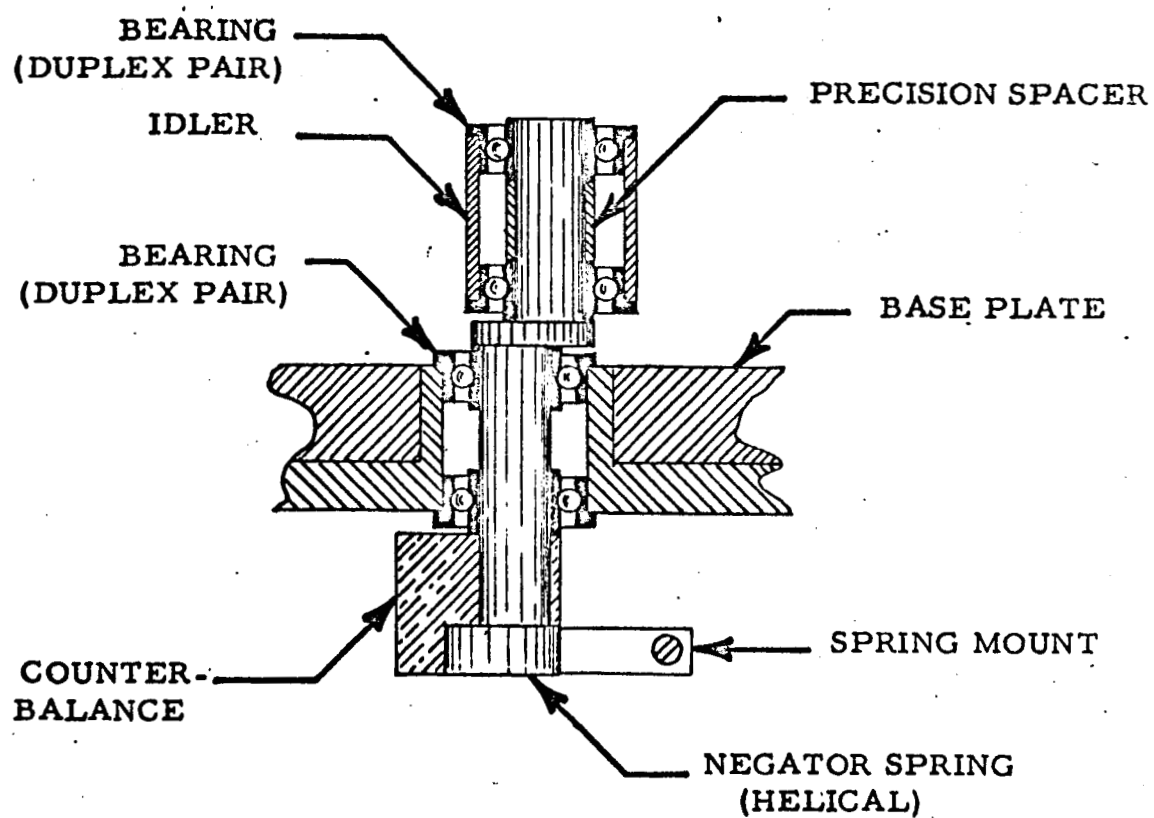
FIGURE 3, ISO-BELT TENSIONING SYSTEM,
6 x 6 CONFIGURATION

FIGURE 4

PRELOADING SCHEMES
6 x 6 CONFIGURATION
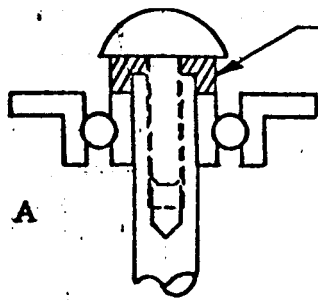
LAPPED SPACER

A

SHIMS

B

SHIMS

C

ADJUSTING SCREW

D

JAM NUTS

E

GLYPTOL   NUT

F
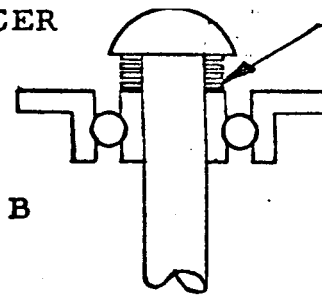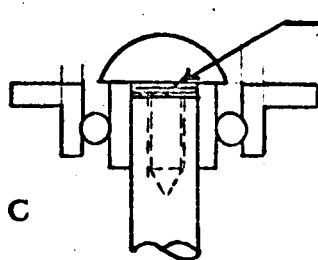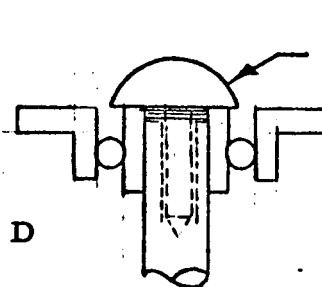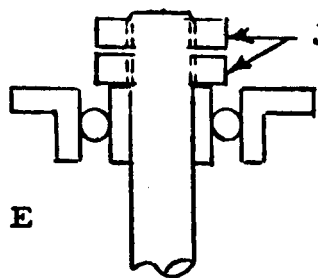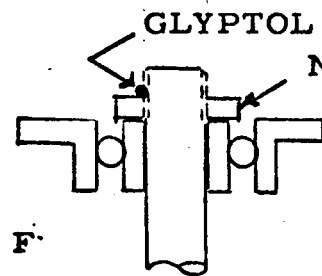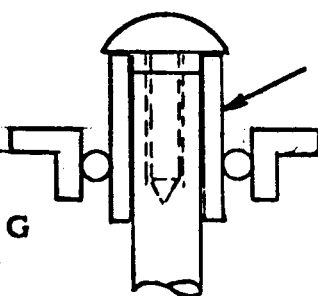
EXTENDED INNER RING

G

H   Use spin-down technique for determining P. L.

P   P

SHRINK FIT

I

13

FIGURE 4. (Continued)

P   P

CLAMP - balanced 2-piece clamp.
Bring surface tured-up
before assembly.

H
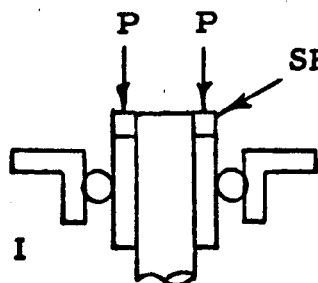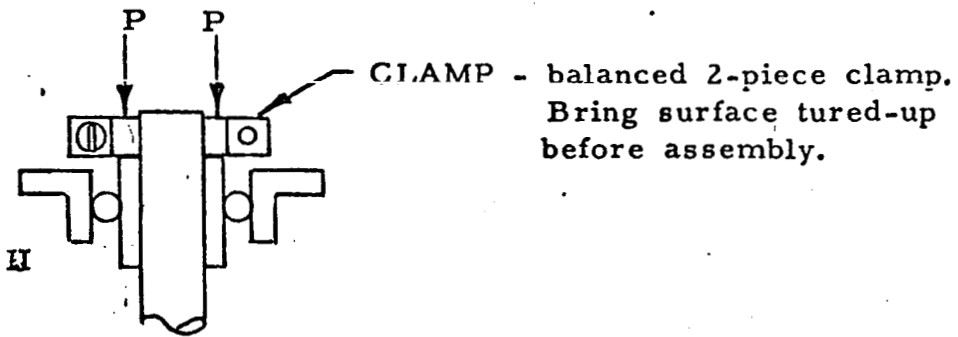
The advantage of extended inner race is that less inner race
misadjustment is possible because of the length of engagement
vs. diameter.

Recommended for proper fit - coded bores and O. D. within
50 microinch bounds.

LAPPED PRECISION SPACER

K
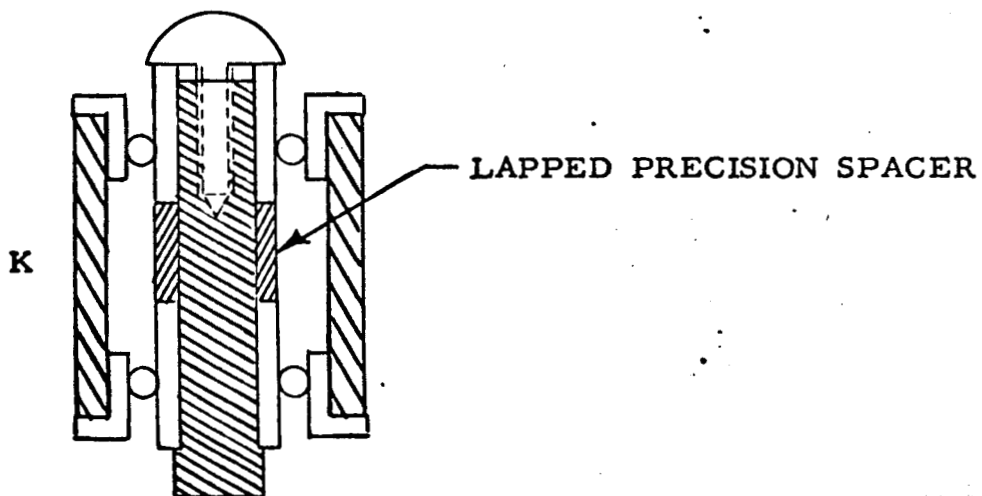
3. 2. 1. 4   Bearing Selection (Continued)

3.   MIL-STD-206 torque traces with each bearing.

4.   Pits and inclusions in raceways would not exceed

0.00005 inch in width.

5.   Bores and outside diameters would be coded in

increments of 0.00005 inch.

6.   High points of eccentricity would be marked on inner

and outer rings.

Both the Barden Corporation and the Reed Bearing Co. felt that 52100

chrome-steel bearings do not present any significant advantage, while having

the disadvantage of being subject to corrosion; a problem with which the Barden

Corporations had had considerable difficulty. All three manufacturers declared

that duplexed bearings do not inherently make for rough bearing operation but

New Hampshire Ball Bearing Co. could torque test duplex pairs and ship

bearings to a specified "hash width" on the torque trace. The Barden represent-

ative indicated that there is no reason why standard production bearings should

not be adequate as evidenced by recent life tests performed by Dr. Clauss on

many of the Barden bearings.

A trip was made to Reed Bearing Company by the Project Engineer in

April 1965. Subassembly drawings were presented for review of bearing

selection and application. It was their view that the installation method was

acceptable but the specific bearing type selected for the tape guides was not

considered to be one of their more reliable bearings. They recommended

replacing the SC-0816-2 with the SC-0820 which has a larger outside diameter.

3. 2. 1. 4   Bearing Selection (Continued)

Their engineers also reommended the use of impregnated phenolic retainers on

the basis that the primary cause of bearing failure is lack of lubrication.

Although nylasint retainers will retain more lubricant this material is subject

to cracking and chipping under load. Therefore it was not recommended. A

Lubricant conforming to MIL-L-6085 is recommended as having excelent

lubricating properties as well as being stable.

Bendix B-10 oil is considered best on the basis of it being the most

contaminant free. With respect to grease lubrication, Bearing Company personnel

indicated that a 20 to 30% fill of Andox E would provide for longer life than any

oil but at the expense of higher torque. Teflon seals are also desirable for

keeping contaminants out but here again torque increases of 10 to 20 times is

expected (under standard test load conditions). In supplying Kinelogic with

the bearings, Reed Bearing Company personnel indicated that they could select

the rings to provide the exact contact angle that is specified instead of the usual

range of radial play which determines a range of contact angle only. With

respect to torque variability (hash width) they said that they could supply the

torque traces on the specific bearings we purchased. They also pointed out that

the Massachusetts Institute of Technology has recently evaluated TCP (Tri

Cresyl Phosphate) as a bearing race coating. TCP has the property of filling

in the low points on a bearing race, which results in a lower running torque

and lower torque variability. There is also available a non-wetting agent which

is applied to the rings but not the races. This prevents lubrication from

"creeping" out of the raceway. Although these two coatings seemed to be

advantageous, it was felt that insufficient field experience did not warrant their

3. 2. 1. 4   Bearing Selection (Continued)

use at the time. Reed Bearing Company personnel indicated that they would

work with us by making available their Talyron machine as well as any other

precision measuring instruments to test the bearing assemblies.

3. 2. 1. 5   Belt Reduction System

In considering the belt reduction system in the light of the Belt Study* an

additional stage of reduction was added so that the driver diameters could be

increased. The increase of driver diameters provides for longer belt life

because of reduced bending stresses. The drive train was optimized by

providing larger driver diameters at the stages with the higher number of stress

cycles per unit time.

It was felt that the increase in the number of belts and bearings will be

offset by a higher MTBF of the belts. Since the limiting element is the life of

the belts, the MTBF of the whole recorder can be expected to increase substantially.

3. 2. 1. 6   Packaging

The following packaging designs were considered for the 6 x 6 configuration:

1. A rubber deck mount with welded end cover.

2. A deck retained by housing halves with

single peripheral weld.

3. A deck retained by housing halves with a

Parker-seal on each half.

4. A single Gasko-seal with deck and covers

fastened by sealed screws.

* Tape Recorder Belt Study, Final Report on Fatigue of Seamless Polyester
  and Polyimide Film Belts.

3.2.1.6   Packaging (Continued)

,   5.   A deck retained by housing halves with a flat

rubber gasket, and sealed securing fasteners.

After considering the above designs, a selection was made which

incorporates the advantages of designs 2 and 4 above.   In the design selected,

the deck is retained by cover halves, using a single Gasko-seal with optional

electronic beam weld.   The fasteners are external to the seal and are also

optional with the welded design.

The layout was planned in consideration of the parameters listed in

"Design Guide for a Spacecraft Tape Recorder" by W. G. Clement, February

19, 1965.   Due to space constraints determined by head size, shielding and

large roller and capstan diameters a 30% overtravel exists in the present design.

In order to assure that excessive deflection of the housing does not occur,

eight tie-down points were incorporated instead of four.   This provides structural

rigidity so that the Gasko-seal does not separate from the mating surface and

thus   loose its sealing capability.

3.2.1.7   Design Review Meeting, 6 x 6 Configuration

On 28 April 1965, a design review meeting was held to evaluate the design

as it existed at that time.   The following salient agreements were reached at

that meeting:

1.   The design would use the JPL drawing

4801264 pressurizing valve.

2.   The clearance between the deck and the

tape pack would be increased to 1/8 inch.

3.2.1.7   Design Review Meeting, 6 x 6 Configuration (Continued)

3.   Anodized aluminum finish was selected

for the ETM housing.

4.,   The design would incorporate electropolished

capstans.

5.   Magnetic heads would be shielded with mu-metal.

6.   The tape guide tollerances were established

as follows:

a) Perpendicularity: $\pm$ 0.0002 inch

b). Height: $\pm$ 0.0005 inch

7.   The bearings selected, Reed type SC-0816-2,

would be used. (See Appendix B)

3.2.2   New Environmental Requirements

After the detail drawings were completed on the 6 x 6 configurations, they
were released for fabrication.   Immediately after release, however, the orders
were cancelled pending a second design review meeting which was held on
9 July 1965.   At that meeting several new requirements were developed.   Process
control drawings, a comparative reliability analysis, a sealing evaluation,
and belt tension measurements are now required.

On 3 August and 13 August 1965, meetings took place which were concerned
with an additional requirement of designing the recorder for a 4400 hour life
with a system probability of survival of 90% at the 50% confidence level.
Preliminary layouts and engineering estimates were made to show the feasibility
of the design approach.   This preliminary work indicates that substantial increase

19

3.2.2   New Environmental Requirements (Continued)

in recording reliability could be achieved by increasing the size to approximately 6 x 8. This would allow larger size pulleys and capstans that reduce the belt stresses and thus increase the belt fatigue life. The larger pulleys also allow for installation of larger bearings which have a higher load rating which is associated with increased life. A reliability analysis is given in Appendix C. A proposal letter was submitted on August 19, 1965 based on increased reliability requirements for the ETM.

As a result of this proposal letter describing the changes required to meet the revised requirements, modifications 1, 2 and 3 to JPL subcontract 951128 were issued. A new design layout was established to replace the 6 x 6 configuration. The new design has dimensions of 6 x 7-3/4 inches.

3.2.3   6 x 7-3/4 Configuration (and other related activities)

3.2.3.1   Mechanical Design Approach

The approach taken in meeting the new requirements was to utilize the features of the 6 x 6 configuration to the greatest extent possible. As can be seen in Figure 5, the 1/2 inch thick deck supports all the bearing cartridges. The bearing cartridges were increased in size to accommodate larger bearings. Labyrinth shields were added to the cartridges as additional protection against bearing contamination. The first and second stage cartridge assemblies were redesigned so that their position could be adjustable. This was necessary because the tolerance on the belt lengths is such that a condition of zero installed stress would result if fixed centers were used on the cartridges. The major task was to optimize pulley sizes, belt wrap angles, and installed

3.2.3.1   Mechanical Design Approach (Continued)

stresses for each of the belts in the system. The new design has three stages

of reduction as shown in Figure 6. This allowed for larger driver pulleys and

increased belt wrap angles in the transmission system which substantially

increases the predicted life of each belt. This more than offsets the fact that

an additional belt and pulley assembly would be a factor in determining the

system probability survival.

3.2.3.2   Electrical Design Approach

The same method of lead termination was used in the 6 x 7-3/4 configur-

ation as was used in the 6 x 6 configuration. As shown in Figure 7, hermetically

sealed headers are used on the lower cover where a pressure differential exists.

Leads from the headers are then routed to connectors which will absorb the

strains of handling.

The leads were placed at one edge of the deck so that the covers could

be swung open without puting stress on the leads, yet without providing

appreciably longer leads.

The leads coming from the head assembly area were routed underneath

the head mounting plate. These leads are nested in a groove put into the tape

deck. An analysis was made comparing the grooved deck with an ungrooved

deck. As can be seen in Appendix D, peak stress of 763 psi is induced at the

groove during a 15 g acceleration loading condition. This far below the yield

point for magnesium (24,000 psi) or even the PEL* point (6000 psi).

*Precision Elastic Limit, C. Jennings and H. S. Brenner, Machine Design,
  April 15, 1965.

3.2.3.3   Belt System Design

A preliminary set of belt calculations was made based on transmitting the full motor torques (0.15 oz-in.) at 75°C. Coefficients of friction of the drive pulleys were established so that all the belt stress ratios would be below 0.9 using the resultant installed stress at an ambient temperature of 25°C which results in a higher installed stress than at 75°C (the upper limit of the operating temperature range). At that time, data on the kinetic coefficient of friction became available as a result of the work done on JPL subcontract 950899. This study reported kinetic coefficients of friction of Mylar in contact with metal pulleys in the range of 0.08 to 0.13. Three of the five belts required a 0.2 kinetic coefficient of friction in order to operate at the required installed stress. A material or method for achieving the 0.2 friction value was investigated. Consideration was given to "Microseal" high friction process 100-1 LL. This process was reported to increase friction from 50% to 300% over bare metal surfaces.

During this period, experience was gained in the application of Kapton ("H" Film). Several belts were fabricated and installed in a recorder which was built by Kinelogic for another application. This experience showed that the shrinkage rate of the material was not sufficiently constant to arrive at a belt size which was reasonably predictable. It would require approximately five belts to yield one of a given length. Secondly the Kapton material showed instabilities after being installed into the recorder, viz., upon initial installation the belt would track on the center of the pulleys but after several days they would mistrack. In addition, residues of yellow powder were deposited

3.2.3.3   Belt System Design (Continued)

on the pulleys and adjacent parts. On the basis of this experience, it was decided to use Mylar rather than Kapton..

Additional data would have to be collected to make a meaningful statistical analysis and such collection and analysis are beyond the scope of JPL subcontract 951128

The belt parameters were finalized based on achieving a 0.2 coefficient of friction on pulleys with Mylar belt material. The predicted life of belts operating at $25^{\circ}C$ using the method given in the belt study is as follows:

Belts	Hours at 95% Conf.
1st stage belt	9,204
2nd stage belt	19,208
3rd stage belt	54,555
Interconnecting belt	59,000
Iso-belt	107,274

Note that these values were not used in making the reliability estimate for the recorder. The values were modified to reflect an extrapolation of the endurance limit curve contained in the Belt Study.*

3.2.3.4   Belt Tension Measurement

A means by which installed belt tensions can be measured was investigated. Non-contacting methods were investigated. These methods are based upon the principle that the natural frequency of a string (or belt) varies with changes in tension. The belt is forced into vibration and the resonant frequency determined

* Tape Recorder Belt Study, Final Report on Fatigue of Seamless Polyester and Polyimide Film Belts.

23

3. 2. 3. 4   Belt Tension Measurement (Continued)

by measuring an abrupt increase in the vibration amplitude. Once the frequency

is known, the tension can be derived from the formula $f = \dfrac{1}{21} \sqrt{\dfrac{T}{m'}}$

where: f = frequency (Hz)

    l = Free length (inches)

    T = Tension (lbs)

    m' = Mass/per unit length (lb. $in^2 sec^2$)

A preliminary experiment was made to determine if a loudspeaker driven

by a signal generator would be a suitable forced vibration source. A belt was

installed between two posts which were mounted on a board. The belt was

apparently under a low tension because it could be seen that one edge of the belt

was slack as compared to the opposite edge. (This belt happened to be curved

in its relaxed state). A frequency sweep was made with the speaker, first at a

low amplitude (approximately 40 dB) and then at a higher level (approximately

75 dB). At the higher level, a displacement of approximately 1/16 inches was

observed. On the basis of this experiment, it was felt that this approach was

resonable.

There are several methods which can be used for detecting the resonant

frequency of the belt. One method is to measure the variability of capacitance

between the belt and a plate. There are commercially made instruments which

are capable of doing this. One is made by Reliance Electric Engineering Co.

and another by the Decker Corporation. Although both of these instruments would

be adequate for sensing vibration amplitude, the budgetary allowance for such

items would not permit their purchase. Another method is to reflect a

24

3.2.3.4 Belt Tension Measurement (Continued)

columated light beam off the surface which would then be channeled to a light sensor by a series of mirrors. It was planned to implement this idea by using a 2-watt zirconium arc lamp which has a beam source diameter of 0.005 inches. The beam would then be set so that it would reflect off of the surface of the belt at an acute angle. It was anticipated that the Mylar surface itself would not be sufficiently reflective. The simplest method is by merely observing with the naked eye the vibration amplitude of the belt while it is being forced into resonant vibration by a loudspeaker. This was the method actually used in adjusting the belt tensions on the ETM recorder. No corelational techniques were used to determine the accuracy of this method. It is felt that this is a subject for future study.

The calculated and measured reasonant frequencies are as follows:

Belt Desc.	Belt lb.	Now in.	Norm Tens. lb.	Belt Thickness (mils)	Belt Width in.	Mass/e lb. sec^2/in^2	Calculated f (cps)
Inter Connecting	13833	1.77	0.092	0.3	.187	7.25×10^{-8}	316
1st Stage	13830	5.4	0.281	0.75	.281	2.72×10^{-8}	300
2nd Stage	13831	3.7	0.251	0.1	.187	2.42×10^{-8}	436
3rd Stage	13834	4.65	0.272	1.5	.218	4.22×10^{-8}	274
Iso-Elastic	13834	4.65	0.272	1.5	.218	4.22×10^{-8}	274

25

3.2.3.4   Belt Tension Measurement (Continued)

and that a low mass reflective material would have to be applied to the belt

surface.   The reflected beam would then be channeled through a series of

first-surface mirrors onto a light sensor so that when the belt is excited at its

resonant frequency and the vibration amplitude of the belt would cause the

reflected light beam to swing beyond the sensitive area of the light sensor.   In

so doing, the output of the sensor would become A.C. instead of D.C.

3.2.3.5   Belt Curvature

One of the major problems encountered in the assembly of the ETM was

to fabricate belts which were straight enough so that the installed stress would

be equally distributed across the full width of the belt.   Several attempts were

made to fabricate a belt using various degrees of tapers on the mandrel.   After

several attempts, a belt was made with sufficient straightness using the

original 1° tape on the mandrel, but under different heat treating conditions.

This belt was cured in the Kinelogic oven instead of the JPL oven, for 1-1/2 hours

instead of 1 hour.   From this experiment it became apparent that in order to

install belts into a recorder at low stresses (approximately 1000 psi) further

study of the fabrication process was necessary so that straightness of belts

could be controlled.   It is believed that one of the controlling variables is the

length to width ratio as well as heat treat temperature and time.   The Iso-belt,

also posed a problem.   The belt width as specified (0.225 wide) would not track on

the center of the tape packs.   With a belt 0.200 wide or narrower improved

tracking was achieved.   The improper tracking of the wider belt is attributed

to the relative width (0.225 vs 0.250) of the belt to the tape pack width.   This is

3. 2. 3. 5   Belt Curvature (Continued)

true because the tape pack is observed to be somewhat concave and thus the edge of the pack acts as a crown to which the belt tries to center itself.

Due to the fact that the two idler rollers are the only crowned rollers in the belt path and the belt span between these rollers and the tape pack is long, their centering effect is not sufficient to overcome the effect that the concave tape packs have. To correct this condition crowns were put on the reel hubs. The effect of these crowns are to allow the tape to comply to the crown thus leaving the tape pack in a convex shape instead of a concave shape.

3. 2. 3. 6   "Micro-seal" Process Evaluation

Verification of the Microseal 100-1 LL was made by actually performing kinetic coefficient of friction tests on the same test equipment used on Contract 950899. Three sets of test pulleys were treated with the Microseal 100-1 LL. One set was 303 CRES, one set was 606IT6 hard anodized aluminum and one set was 6061 T6 without a prior treatment. Torque-creep curves were then obtained by the same procedure which was employed in the Belt Study.* Each set of pulleys received four test runs at installed tensions ranging from 543 psi to 8400 psi. The comparative friction values of the three materials is shown below:

Pulley Treatment	Coefficient of kinetic friction		
	303 CRES	606IT6	606IT6 Hard anodized
None	0. 075	-	0. 12
Microseal 100 1 LL	0. 20	0. 27	0. 23

* Tape Recorder Belt Study, Final Report on Fatigue of Seamless Polyester and Polyimide Film Belts.

27

3.2.3.7   Sealing Evaluation

The principle of electron-beam welding is the application of a high
energy focused electron-beam to reactive metals.   When the subject is
bombarded with a dense stream of high-velocity electrons, virtually all of the
kinetic energy of the electrons is transformed into heat upon impact.

The method commonly used to hermetically seal tape recorder mechanisms
is to compress elastomer devices such as 0 rings or Gasko-seal.   The use
of Gasko-seal have been successful on recorders built for JPL programs
but they have required a high degree of quality control to assure the inherent
low leakage rate that is required.   A brief investigation was made to determine
if electron-beam welding methods would offer any advantage.   Electron-beam
welding usually takes place in an evacuated chamber with the beam generating
and focusing devices and the subject being in a vacuum environment.   Welding
in a chamber imposes several limitations, but at the same time provides one
important advantage viz., an inert environment in which the metal may be
welded without fear of chemical contamination.   Another advantage of electron-
beam welding is the capability to make exceedingly narrow, deeply-penetrated
welds.   A housing was designed and a detailed drawing was made which is
included as an optional cover on the ETM parts list.   A meeting was held at
the North American Aviation welding facility to obtain specific experience in
welding the ETM housing.   Appendix E is a report of the discussions at that
meeting.

3.2.3.8 Bearing Application

After reviewing the information gained in bearing application, specifications were prepared for each type of bearing used in the ETM. A summary of these specifications is given in Appendix G.

The procurement of bearings to these specifications presented a delivery problem. Twenty to twenty-two weeks delivery was quoted by NHBB Co., and Reed BB Co. This delivery schedule precluded the use of these bearings, so standard bearings were purchased with a 0.0007 to 0.0009 inch radial play. These bearings were then tested and torque traces per Mil Std. 206A prepared. See Appendix F for torque traces.

Two methods of preloading bearings were attempted. First a fixture was made up which was to measure the distance between one end of the outer race with respect to the inner race within ± 0.00002 (See Figure 8) under a given load. This fixture did not operate properly because the bearing outer race would shift radially as well as axially.

The second method of preloading was to measure rundown time of the unloaded bearing and then measure the rundown time of the loaded bearing. The preload is increased incrementally by lapping the inner ring spacer until a predetermined percentage of unloaded rundown time is achieved. This percentage is determined for each bearing by referring to typical axial load vs torque curves which are characteristic for each size bearing. Characteristics for the various bearings are as follows:

3.2.3.8 Bearing Application (Continued)

Application	Assy No.	Brg Size	Run Down Time (Sec)		Breadkaway Torque (oz-in)		Equivalent Preload Lbs.
			Unloaded	Preloaded	C. W.	C. C. W.	
Tape Reel Assy Feed	C13844	SFR 4	16	3-4/5	.007	.007	3
Tape Reel Assy Take up	C13844	SFR 4	21-2/5	4-1/5	.008	.008	3
1st Stage Speed Reduction	C13850	SFR 3	5	2	.006	.006	1
2nd Stage Speed Reduction	C13851	SFR 3	5-1/5	2-3/5	.004	.004	1
Slow Capstan Assy	C13949	SFR 3	10-3/5	4	.005	.005	1
Fast Capstan Assy	C13848	SFR 3	17-3/5	7-4/5	.005	.005	1
Iso-Belt Idler Assy	C13846	SFR 3	6-3/5	3-2/5	.004	.004	1
Tension Arm Assy Roller	C13847	SFR 3	6-1/5	2-3/5	.005	.005	1
Tape Guide Roller	C13853	SFR 2-5	N/M	N/M	N/M	N/M	1
Tension Arm Pivot	C13847	SFR 188	N/M	N/M	N/M	N/M	1

3.2.3.9 End-of-Tape Sensors

The end-of-tape sensors incorporated in the ETM are based on a previous design used for the miniaturization recorder, JPL subcontract 950850. A neon bulb flashes periodically which energizes one of two silicon solar cells. Each end-of-tape has the oxide removed on half the tape width for approximately one foot. One end-of-tape has the oxide removed on the top and the other end on the bottom.

30

PRELOAD WEIGHT

INNER ROW
SUPPORT

BEARING
SPECIMEN

X

REFERENCE SURFACE
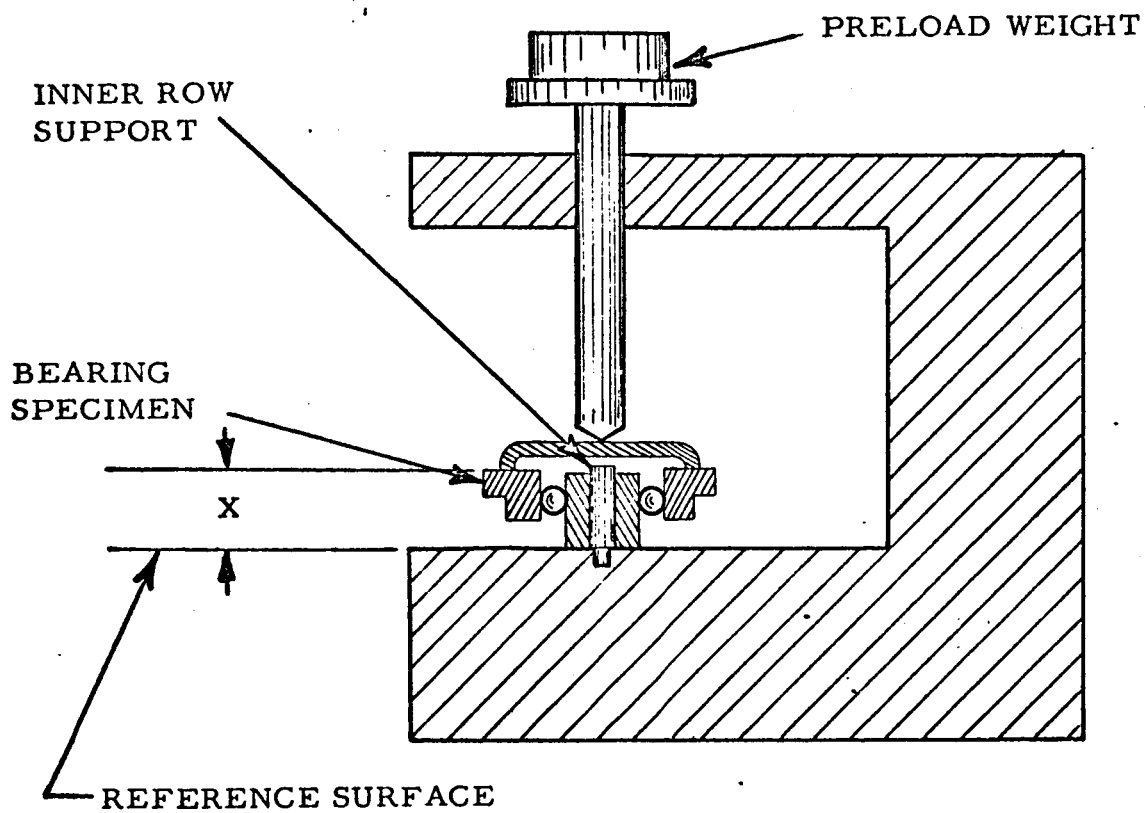
Distance x is to be measured within $\pm$ 20 micro inches.

PRELOAD FIXTURE

FIGURE 8

31

3.2.3.9 End-of-Tape Sensors (Continued)

Each solar cell is placed opposite one of the two tape windows, thus indicating which end-of-tape is being sensed. A General Electric A 1C bulb is used, which has a life rating of 25,000 hours continuous duty. Based on its duty cycle of $2.5 \times 10^{-5}\%$ the useful life is expected to be many times the life at continuous duty. The solar cells used are Hoffman type No. 52C which have approximately four times the power output than the previously used No. 55C.

3.2.3.10 Flutter

The initial flutter tests performed on the unit disclosed that excessive flutter (8% p-p) was present as shown in Figure 9. The flutter frequency observed was in the 0.5 to 1.5 Hz range, which correlated to the capstan, tape pack and idler rotational rates. The eccentricity of the fast capstan was measured to be 0.0007 TIR which theoretically produce tape speed variations of about 0.5%. Interconnecting belt transmissability was tested and it was found capable of transmitting 3 oz-in of torque which is more than sufficient. During this initial test, the Iso-belt was observed to be tracking off the edge of the tape pack. After correcting this condition further flutter measurements were made and the flutter was 6% to 8% p-p. The FM envelope on the low frequency component was no longer present, but a 300 Hz component was observed and measured with an electronic frequency counter. This frequency is twice the motor drive frequency (150 Hz). At this point, it was felt that the motor was not being driven properly. The motor which was wound for square-wave operation was being driven with a sine-wave. To correct this, a two-phase square-wave power source was provided. This reduced the flutter when measured to 3% p-p.

32

3.2.3.11   Reliability Program

A reliability estimate for the ETM Recorder was prepared to indicate the probability of performing adequately for a 4400 hour mission. As mentioned previously, the belt data had to be handled in a special manner in order to predict belt lifetimes. The report* combines the failure rate predictions of belts and bearings in assessing the probability of survival of the recorder which was found to be 0.9292 at the 50% confidence level for a 4400 hour period in a space environment.

In addition to the reliability analysis*, a comparative analysis between the Mariner C recorder designed by Raymond Engineering and the ETM unit was made. The report demonstrated that the reliability of the Raymond unit is significantly less than the ETM and that this is attributable to the high stress levels at which the belts are operated.

3.2.3.12   ETM Performance Characteristics

The ETM Recorder was tested in accordance with the system test procedure. The salient performance characteristics are as follows:

1.   Flutter - 3% peak-to-peak, 0.1 to

10,000 Hz bandpass.

2.   Start-Stop Time - 25 milliseconds start
                                    100 milliseconds stop

3.   Output Level - .16 millivolts

4.   Signal-to-Noise Ratio - 50 db

* Reliability Analysis of Tape Recorder Model ETM, by A. H. Cronshagen, Kinelogic Corporation for JPL.

33

3.2.3.12   ETM Performance Characteristics (Continued)

    5.   End-of-Tape - Start-of-Tape Sensor Level

                EOT - 240 millivolts

                SOT - 130 millivolts

    6.   Sensor Crosstalk - 27.5 db at EOT

                28 db at SOT

    7.   Power - Minimum running = 10 volts, 100 milliamps

                            = 1 watt

          Average running = 14 volts, 180 milliamps

                          = 2.5 watts

34

3.3 CONCLUSIONS

In conclusion it may be said that several significant advances in the art of high-environment tape recorder design have resulted from JPL subcontract 951128. The sailent conclusions which may be drawn as a result of this program are:

1. It is possible to design and build a recorder which has the characteristics specified in the subcontract and complys with the specifications of reliability and environment.

2. The recorder as designed has an estimated reliability for 4400 hours of 0.9292 at a 50% confidence level with tape speed of 4 ips.

3. Tape speeds of 1, 2, 4 and 8 ips may be obtained within the ETM configuration.

4. Although the electron-beam welding process for hermetic sealing of the recorder housing results in a package with a leakage rate far beyond the estimated life of the ETM, the difficulty in servicing the unit makes this process undesireable.

5. The predicted life of a recorder is primarily a function of belt life.

6. Further study of the belt fabrication process is necessary to provide understanding of all the forces involved.

35

7.   In order to attain the predicted belt life,
     a coefficient of kinetic friction of 0.2 is
     required.

8.   Further study of the friction between belts
     and capstans should be made.

9.   Further study of the method of measuring
     the belt tension under dynamic conditions
     should be made.

10. Further study of the fabrication of Kapton
     belts should be made.

36

NEW CONCEPT IN HIGH RELIABILITY TAPE RECORDERS FOR SPACEBORNE DATA STORAGE

By D. L. Burdorf

37

NEW CONCEPT IN HIGH RELIABILITY TAPE RECORDERS FOR SPACEBORNE DATA STORAGE

By D. L. Burdorf

Summary. - The need for large bit capacity in on-board data storage for deep-space probes, spacecraft, satellites, and aircraft, has created a requirement for a tape recorder of ultra-high reliability.

In an ideal recorder, the conventional capstan would be eliminated and the reels would be driven such that the linear velocity and the tension of the tape between reels would be constant from the beginning to the end of the reel. The heads would also be the only elements in contact with the tape. Reliability would be enhanced by driving the reels, rather than the tape, through a reduction in the number of moving parts. Reducing the number of elements in contact with the tape would also increase tape life.

The Iso-Elastic Drive, closely approaches the ideal recorder drive system. The reels are driven by a seamless polyester belt which is in direct contact with the periphery of the tape reel. The belt is driven at constant linear velocity (resulting in low flutter) and in such a manner that it generates a constant tension in the tape connecting the two reels and passing across the heads.

Constant tape tension in a high-reliability recorder is necessary in order to optimize 1) tape tracking and guidance, 2) effective bias level on the tape during direct-type recording, 3) playback level, 4) head wear, and 5) drop-outs. The Iso-Elastic Drive reduces the number of moving parts by approximately 30% as compared with conventional recorders. The tape drive has the additional desirable characteristic of operation equally well in either direction.

Introduction. -Developing a tape recorder for space missions necessitates a design of tape transport and associated electronics which can withstand extreme environmental conditions while offering very high reliability. This problem is complicated by the demand for faithful reproduction of the recorded data, and by unusually small weight, volume, and power consumption limitations. Previous approaches to these problems have employed various techniques of component selection to reduce the envelope and power consumption to an acceptably small level, while essentially maintaining a design originally developed for ground station use.

In order to obtain maximum accuracy of reproduction, ground station tape recorders have used complex reeling systems including several motors, clutches, springs, Servo systems and frequently pneumatically operated brakes and sensing devices. The complexity of the design of ground oriented tape recorders creates an inherent reliability problem because of the many subsystems that must operate concurrently. At ground stations, reliability is easily obtained by endless redundancy of equipment whose weight,

1. The Iso-Elastic Drive is a Kinelogic proprietory concept and development. A patent application in the names of D. L. Burdorf and J. T. Blakistone is the property of Kinelogic Corporation.

I

38

volume and power consumption are only limited by economic constraints. Thus, it may be seen that the complexity necessitated by accuracy of reproduction is the antithesis of reliability.
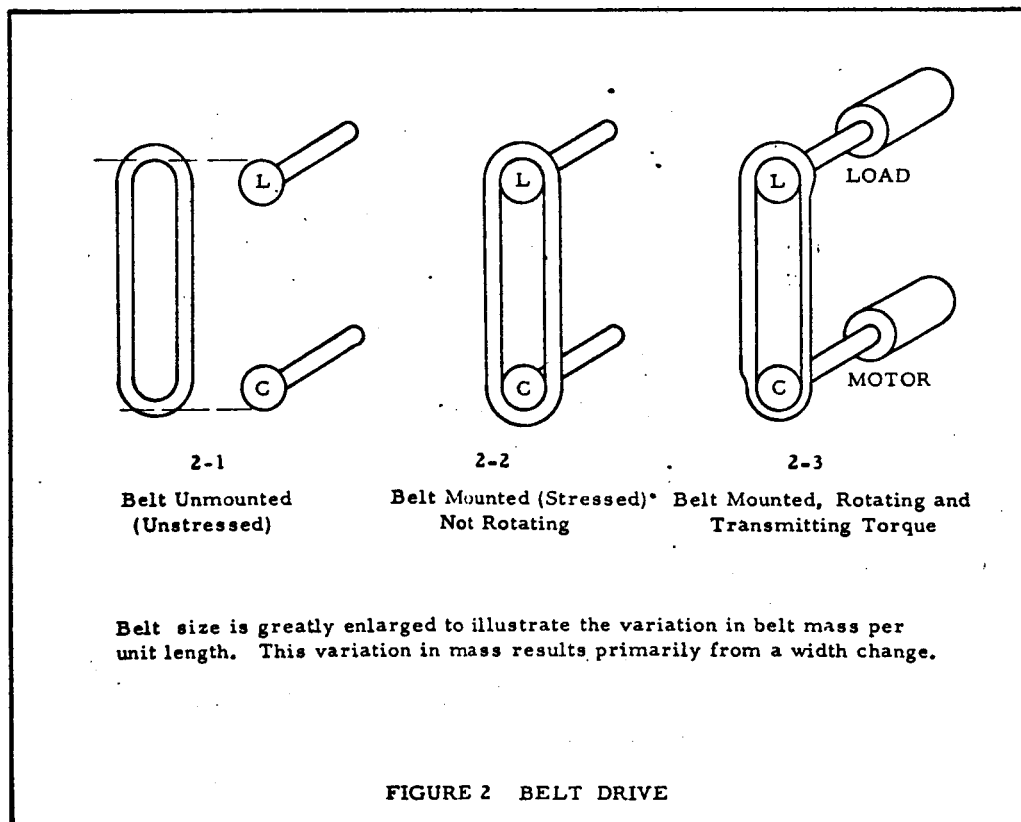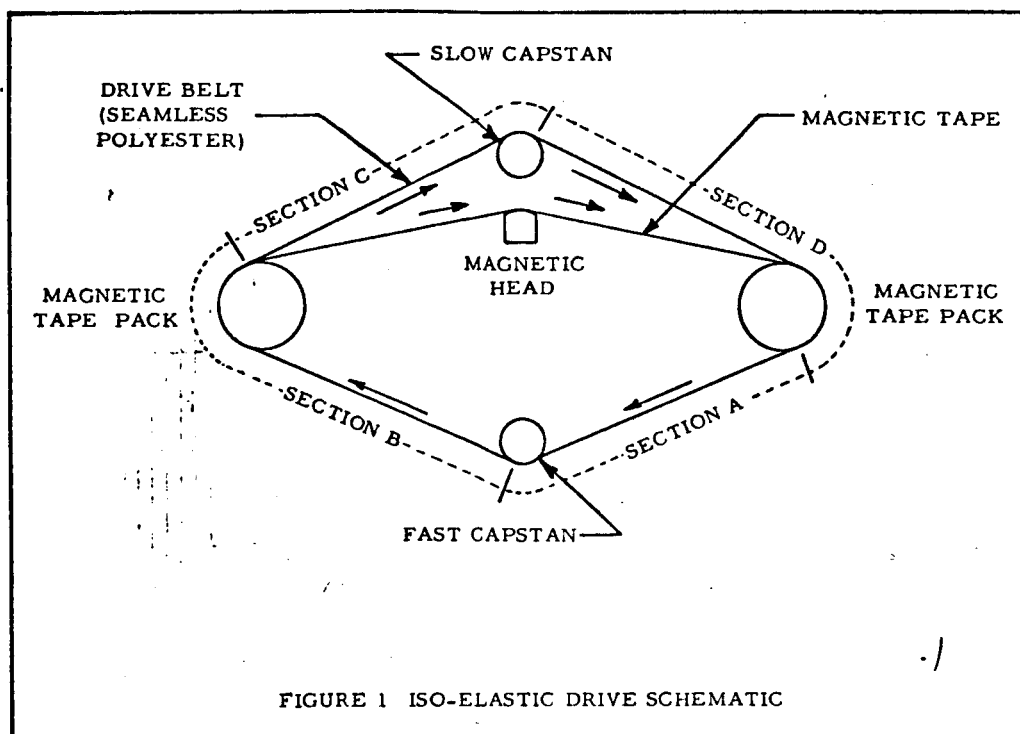
This paper discusses a new concept in tape recorder design for space and related applications which uses the Iso-Elastic Drive principal of peripherally driving the tape packs to obtain high reliability and excellent reproducibility in a simplified reeling system having small size, low weight and minimal power consumption requirements.

Iso-Elastic Drive. - Transferring magnetic tape from one reel to another at essentially constant velocity and tension is a basic requirement for any high quality instrumentation type magnetic tape recorder. Essentially constant velocity is the equivalent of very low flutter which is necessary if distortion (spurious frequency generation) is to be avoided. The need for constant tape tension, however, is not so apparent. For example, some flutter frequency components are a function of the tape tension. Tape tracking and guidance, effective bias level on the tape during direct type recording, playback level, head wear, drop-outs, etc. are all influenced by tape tension. Difficult problems are encountered, however, in meeting this requirement. The difficulty stems from the fact that the diameter of each reel is constantly changing. To achieve constant tape velocity, the conventional approach is to insert one or two capstans between the reels to provide metering of the tape. Tape tension controls run the gamut from constant torque braking and take-up of the reels to very sophisticated Servo systems. The more precise systems use either reel Servos or a differential capstan drive. In a differential capstan drive tape tension is generated primarily by the two capstans and reel torques are reduced to as low a value as practical. Variations in the reel torques are therefore relatively small when compared to the tension generated by the capstans and do not cause large tape tension variations.

In an ideal system, the reels would be driven such that the linear velocity and the tension of the tape between the reels would be constant from the beginning to the end of the reel. The heads would be the only element in contact with the tape during the transfer of tape from one reel to another, thus reducing the number of flutter generating elements to a minimum.

The Iso-Elastic Drive closely approaches the ideal solution. The reels are driven by a seam'ess polyester belt riding directly on the outer layer of tape in each reel. The belt is driven at constant velocity and in such a manner that it generates a constant tension in the tape connecting the two reels. Thus, the two prime requirements are accomplished in the Iso-Elastic Drive without the use of a Servo.

The basic configuration of the Iso-Elastic Drive is illustrated in Figure 1. The operating principle is based on drive belts mechanics which are commonly misunderstood. For example, the fact that a driven pulley rotates at a speed slightly slower than indicated by conventional calculations is generally attributed to belt "creep" around the pulley. Analysis reveals that this is not "creep." This speed variation is due to the belt running at different speeds as it travels over different speeds as it travels over different pulleys in the system. This pheno-

3.

3⁷

FIGURE 1 ISO-ELASTIC DRIVE SCHEMATIC

Labels in figure:
- SLOW CAPSTAN
- DRIVE BELT (SEAMLESS POLYESTER)
- MAGNETIC TAPE
- SECTION C
- SECTION D
- MAGNETIC HEAD
- MAGNETIC TAPE PACK
- MAGNETIC TAPE PACK
- SECTION B
- SECTION A
- FAST CAPSTAN

2-1
Belt Unmounted
(Unstressed)

2-2
Belt Mounted (Stressed)
Not Rotating

2-3
Belt Mounted, Rotating and
Transmitting Torque

LOAD

MOTOR

Belt size is greatly enlarged to illustrate the variation in belt mass per
unit length. This variation in mass results primarily from a width change.

FIGURE 2   BELT DRIVE

menon is illustrated in Figure 2. In Figure 2-1 the belt is shown in a non-stressed condition before mounting. When the belt is mounted as shown in Figure 2-2, an initial tension is developed as a result of stretching the belt over the pulley system. This stretching reduces the dimensions of the belt cross-section since the length has been increased. Figure 2-3 shows the pulley system transmitting torque. In a conventional belt system where the initial tension is sufficient to prevent belt-pulley slippage, only one of the two belt sections between the two pulleys transmits the torque. The additional force present in this section of the belt results in further belt elongation, as illustrated in Figure 2-3. As this elongated section comes off the driver, the load tension is no longer present. As a result, belt contraction takes place in the no-load side. It should be noted that for the belt section under load, essentially no elongation takes place until the belt elements come free of the load pulley, nor does the contraction of the belt on the no-load side occur until belt elements leave the motor drive pulley. This is due to the fact that the belt is under sufficient pretension to drive without slip.

Since the belt mass passing a given point anywhere in a belt system per unit time must be constant for a condition of equilibrium, it follows that the linear speed of the belt on its load side must be greater than that on its no-load side. Thus, a belt under load can run without slip while having its load and no-load sides running at different linear speeds. A properly designed pulley system can have a wide range of loads over which an equilibrium condition exists without belt slippage. It can be shown that such conditions are practical, using conservative design stresses. These facts are essential to understanding the Iso-Elastic Drive.

In a recorder, the pretensioned seamless polyester belt (Reference Figure 1), is simultaneously driven by both the slow capstan and the fast capstan, the fast capstan having a surface speed a few tenths of a percent faster than the slow capstan. The belt pretension is sufficient to prevent slippage on either drive capstan or either tape pack under any conditions. In Figure 1, "B" is the take-up tape pack and "A" is the supply tape pack. The difference in surface speed between the fast and slow capstans tend to elongate the drive belt in Sections A and D. This elongation occurs because belting is removed by the fast capstan faster in Sections A and D than it is paid out by the slow capstan. The stretching reduces the belt cross-section as shown in Figure 2-3. The result is a higher linear speed (and tension) in this area (sections A and D). By the same token, the fast capstan is paying out belting into sections B and C faster than it is being removed by the slow capstan from these sections. The consequent belt contraction shows up as a slower linear speed (and lower tension) in these sections. The difference in capstan speeds simulates a loaded pulley system.

Due to the fact that the drive belts are coupled in non-slip fashion to magnetic tape packs A and B which are themselves interconnected by the magnetic tape, the tendency of Section D to run faster and of Section B to run slower is neutralized by tension developed in the magnetic tape.

The principle of operation described above is dramatically demonstrated by using an operating system and purposely introducing a slack loop of tape between the reels. The slack is removed and the proper tape tension is re-established in a matter of seconds. Due to its

symmetry, the Iso-Elastic Drive also has a very desirable feature for many applications. Reversal of tape motion and reeling conditions can be accomplished by merely reversing the directions of rotation of both capstans.

The mathematical analysis of the Iso-Elastic Drive shows that desired operating parameters can be established with very conservative belt and bearing loads, thus assuring a long operating life.

Power requirements are extremely low, the major portion being used to overcome bearing friction and magnetic tape-head friction.

One of the more significant advantages of the Iso-Elastic Drive is the complete absence of reel brakes, clutches, motors, springs, etc. which constitutes a large percentage of the moving parts in a conventional recorder. It is usually possible to reduce the number of rotating parts to about one-third by using the Iso-Elastic Drive. This makes it possible to achieve a considerably higher degree of reliability which is so important in instrumentation recorders.

Analysis of the Iso-Elastic Drive. - The following is a treatment of the mechanics involved in a recorder employing the Iso-Elastic Drive. In Part I, the relations between belt tensions, wrap angle, coefficient of friction, and transmitted power are developed. In Part II, these relations are combined with tension and velocity conditions to produce the essential tape speed, tape tension, and power equations. Parts III and IV consider variations in the system as the tape is transferred from supply to take-up reel. Part V considers the properties and life of the polyester belts. Part VI discusses the effect of introducing magnetic heads into the system, and includes an actual example.

(Continued next page)

Part I, Analysis of Conditions to Prevent Belt Slip (Single Capstan)

Assume that the belt does not slip on the capstan. This requires that the friction forces between the belt and the capstan be large enough so that they can produce the change of tension. Consider a differential arc length over the contact region as shown in Figure 4.

F_n = Normal component of force = $T d\theta$

F_p = Parallel component of force = $dT - F_f$

F_f = Friction force = μF_n = $\mu T d\theta$

If the belt is just at the slip - no slip condition and not accelerating, then:

F_p = 0 = $dT - \mu T d\theta$

Integrating from T_1 to T_2 and θ_1 to θ_2 in the direction of ω, we get

$$\frac{T_2}{T_1} = e^{+\mu\theta_0} \text{ for } T_1 > T_2$$

$$\frac{T_2}{T_1} = e^{-\mu\theta_0} \text{ for } T_1 < T_2 \qquad (1)$$

Therefore, the no slip condition requires

$$\theta_0 \geq \frac{1}{\mu} \left| \log e \frac{T_2}{T_1} \right|$$

For a steady state solution in which the belt does not either break or pile-up on the capstan, the mass per unit time of belt entering and leaving the capstan must be equal. Since the mass per unit time is the velocity times the mass per unit length:

$$V_1 P_1 = V_2 P_2 \qquad (2)$$

If tensions do not exceed the belt's elastic limits, using Hooke's law we get,

$$P_2 = \frac{P_1}{1 + \dfrac{T_2 - T_1}{K + T_1}} \qquad (3)$$

where $K = EA$

Now Let

$$T_c = T_2 - T_1$$

If $T_2 > T_1$, the capstan is driven, if $T_1 > T_2$, the capstan is driving $\qquad (4)$

From equations (3) and (4)

$$T_c = (K + T_1) \left(\frac{P_1}{P_2} - 1 \right) \qquad (5)$$

43

A ▫ belt cross section area

E = Young's modulus of belt

V = velocity of the center of the belt

P = mass per unit length along the belt

T = tension in the belt

r = radius of the capstan

† = thickness of the belt

ω = angular velocity of the capstan

θ_o = angular distance over which the belt contacts the capstan

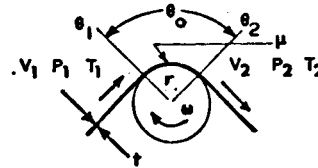μ = coefficient of friction between the belt and the capstan
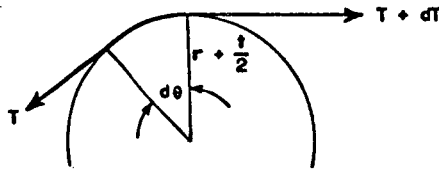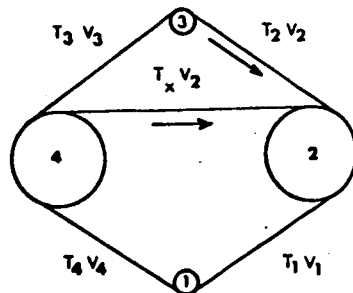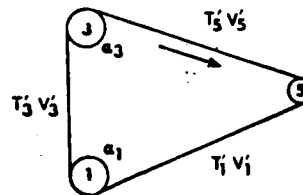

FIGURE 3 DRIVE BELT OVER CAPSTAN

FIGURE 4 DIFFERENTIAL ARC OF DRIVE BELT CONTACT AREA OVER CAPSTAN

Bottom

Top

$$\alpha = \frac{\text{Bottom radius}}{\text{Top radius}}$$

FIGURE 5 DRIVE BELT DIAGRAM, TOP AND BOTTOM

Using (2) in equation (5), and since normally $K >> T_1$,

$$T_c = (K + T_1) \left(\frac{V_2}{V_1} - 1\right) \approx K \left(\frac{V_2}{V_1} - 1\right) \tag{6}$$

To prevent a belt from slipping, a pretension T_o is applied where

$$T_o = \frac{T_1 + T_2}{2} \tag{7}$$

Combining equations (7) and (1), one obtains, for the minimum pre-tension required in order to obtain a tension T_c without slipping:

$$T_o = \frac{T_c}{2} \left(\frac{1 + e^{\mu\theta_o}}{e^{\mu\theta_{o-1}}}\right) \tag{8}$$

Part II, Analysis of the Iso-Elastic Drive System

All belts are assumed not to slip and thus have a velocity equal to the pitch velocity of the take-up reel or capstan. The frictional losses of reels, capstan bearings, and heads will be neglected. For a steady state solution, the net force and torque must be zero and thus:

$$T_4 = T_3 + T_x \tag{9a}$$

$$T_1 = T_2 + T_x \tag{9b}$$

$$T_3 - T_2 = a_3 (T'_5 - T'_3) \tag{9c}$$

$$T_4 - T_1 = a_1 -(T'_1 - T'_3) \tag{9d}$$

Also:

$$V'_3 = a_3 V_3 \tag{10a}$$

$$V'_1 = a_1 V_1 \tag{10b}$$

According to equations (9a) and 9b), the tension in the tape is:

$$T_x = T_4 - T_3 = T_1 - T_2 \tag{11}$$

From equations (6) and (11): (Remembering that (6) was developed for $V_2 > V_1$ and here the subscripts signify different values)

$$K_b \left(\frac{V_1}{V_2} - 1\right) = -K_b \left(\frac{V_3}{V_4} - 1\right) \tag{12}$$

Note here, the (1) sign proceeding the $\frac{V_3}{V_4}$ term. This appears because the original equation (6) was derived for the pulley being driven by the belt. Here we have the opposite situation for $T_4 - T_3$.

If the tape is inelastic or pretensioned so that it does not stretch:

$$V_2 = V_4 \tag{13}$$

8

Substituting in (12):

$$V_2 = \frac{V_1 + V_3}{2} = \text{Tape Speed} \qquad (14)$$

From equations (12) and (14),

$$T_x = K_b' \left(\frac{V_1 - V_3}{V_1 + V_3} \right) = \text{Tape Tension} \qquad (15)$$

Thus, the tape speed and tension depend only on the capstan velocities and the elastic properties of the belt, and not on reel radius.

By applying equations (6), (9), (10) and (14), the speeds V_1 and V_3, (and thus the tape tension and speed,) can be related to the motor speed and the elastic properties of the capstan drive belt. In the usual case, when the capstan drive belt does not stretch, then:

$$V_1' = V_3' = V_5' = \text{speed of motor driven capstan} \qquad (16)$$

and by equations (10a) and (10b):

$$V_3' = \frac{V_5'}{a_3} \qquad (17a)$$

$$V_1 = \frac{V_5'}{a_1} \qquad (17b)$$

From equation (13) and equations (17a) and (17b)

$$V_2 = \frac{a_1 + a_3}{2 \, a_1 \, a_3} \, V_5' = \text{Tape Speed} \qquad (18)$$

and from equations (14), (17a) and (17b):

$$T_x = K_b \left(\frac{a_3 - a_1}{a_3 + a_1} \right) = \text{Tape Tension} \qquad (19)$$

Considering the tension at the capstans, the power to drive the tape is:

$$P = V_1 (T_1 - T_4) + V_3 (T_3 - T_2) \qquad (20)$$

Using equation (11) and assuming $T_4 \approx T_2$

$$P = T_x (V_1 - V_3) \qquad (21)$$

and from equation (21) and (15), eliminating V_3, we get

$$P = \frac{2 T_x^2 V_1}{T_x + K_b} \approx \frac{2 T_x^2 V_1}{K_b} \qquad (22)$$

For a given tape tension and velocity, the power is inversely proportional to K_b or $E_b A_b$ and minimum power is obtained with an infinitely stiff belt. Practical considerations require the belt to have a modulus of elasticity in the region of 10,000,000 lb/in^2 or less.

Part III, Addition of Tensioning Idlers. - A simple Iso-Elastic belt path was shown in Figure 1 and analyzed in Parts I and II. To compensate for different amounts of magnetic tape and to allow replacement of reels of tape, it is desirable to use a tension idler in one section of the Iso-Elastic belt path. The tension idler acts to take up drive tape to produce a fixed tension in the section of the Iso-Elastic drive belt it acts on. The tensions in the other three sections will take values differing from this fixed value by amounts shown in the analysis on the preceding pages.

Part IV, Analysis of Dynamic Characteristics. - This analysis thus far has neglected the fact that as the system runs the tape packs change size, causing a repositioning of the drive belt. Consider Figure 6.

From the diagram it is clear that in the initial state the total length of the drive belt on the feed (left) side of the capstans is longer than the total length on the take-up (right) side. In the later state, however, after the tape has been transferred, the situation is reversed, with more drive belt on the right than on the left.

It will be shown that as the tape is transferred, a small increase in tension is created in the belt on the right side and a small decrease in tension is created on the left side, causing these tensions to differ slightly from the values calculated earlier. The process by which the belt is transferred from the left side to the right can then be explained in terms of these changes in tension, with no belt slip taking place on the capstans or the tape packs.

The Length of Belt between capstans is divided into three portions:

$$L_b = L_{T_a} + L_{T_b} + L_w \tag{1}$$

where

$$L_{T_a} = \sqrt{D_a^2 - (R - r_a)^2} \tag{2}$$

$$L_{T_b} = \sqrt{D_b^2 - (R + r_b)^2} \tag{3}$$

$$L_w = R\phi \tag{4}$$

then

$$dL_b = dL_{T_a} + dL_{T_b} + dL_w \tag{5}$$

$$= \frac{-(2R - 2r_a)\, dR}{2\sqrt{D_a^2 - (R - r_a)^2}} + \frac{-(2R + 2r_b)\, dR}{2\sqrt{D_b^2 - (R + r_a)^2}} + R d\phi + \phi\, dR$$

47
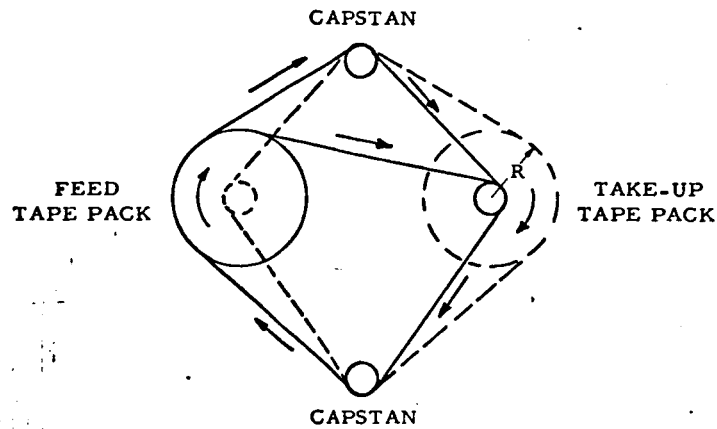
NOTE
Solid lines show packs in initial state,
dotted lines after tape transfer.

FIGURE 6   ISO- ELASTIC DRIVE SYSTEM SHOWING CHANGING TAPE PACK RADII

FIGURE 7 ANALYSIS OF TAPE REEL WITH ASSOCIATED CAPSTANS

but

$$d\phi = d\phi_a + d\phi_b \tag{6}$$

$$t\,dl = 2\pi R\,dR \qquad (l \text{ is length of tape}) \tag{7}$$
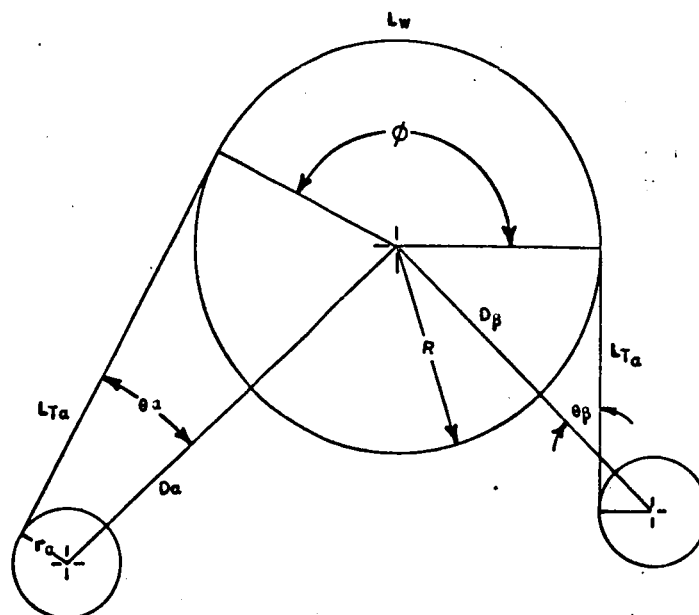
$$d\phi_a = \frac{dR}{L_{T_a}} = \frac{t\,dl}{2\pi L_{T_a} R} \tag{8}$$

$$d\phi_b = \frac{dR}{L_{T_b}} = \frac{t\,dl}{2\pi L_{T_b} R} \tag{9}$$

substituting equations 2, 3, 7, 8, and 9

$$dL_b = -\left(\frac{R-r_a}{L_{T_a}} - \frac{R+r_b}{L_{T_b}} + \phi\right)\frac{t\,dl}{2\,R} + R\left(\frac{t\,dl}{2\pi L_{T_a} R} + \frac{t\,dl}{2\pi L_{T_b} R}\right) \tag{11}$$

$$\frac{dL_b}{dl} = \frac{t}{2\pi}\left[\left(\frac{1}{L_{T_a}} + \frac{1}{L_{T_b}}\right) - \left(\frac{1}{L_{T_a}} + \frac{1}{L_{T_b}}\right) + \frac{1}{R}\left(\frac{r_a}{L_{T_a}} + \frac{r_b}{L_{T_b}} - \phi\right)\right] \tag{12}$$

$$\frac{dL_b}{dl} = \frac{t}{2\pi R}\left[\frac{r_a}{L_{T_a}} - \frac{r_b}{L_{T_b}} + \phi\right] \approx \frac{dl}{dL_b} \tag{13}$$

This represents the increase in belt travel per unit of tape travel as the tape pack builds up. Since the capstans run at synchronous speed and the values are so small, this also represents the decrease in tape speed at this point in the tape pack. The other reel has an increase in tape speed at its complementary point in the tape pack. The tape speed at the head is the average of the increase and decrease on the two reels. If the differing layouts on both reels are considered as a negligible difference, the increase can be calculated at the full and empty reel conditions and the average of the increase at full reel and the decrease at empty reel will be the maximum variation from the nominal speed which occurs at the mid-reel condition. In a typical recorder:

	Full Reel	Empty Reel
LT_a	1.9 inches	2.7 inches
LT_b	0.5 inches	2.3 inches
ϕ	$216° = 3.77$ rad.	$132° = 2.30$ rad.
t	0.00117 inches	
$r_a = r_b$	0.1250 inches	
R	2.35	1.0

49

Full Reel

$$\frac{dl}{dL_b} = \frac{.00117}{2\pi \ 2.35}\left(\frac{.125}{1.9} - \frac{.125}{.5} + 3.77\right)$$

$$= \frac{.000668}{2.35} = .000282$$

Empty Reel

$$\frac{dl}{dL_b} = \frac{.00117}{2\pi}\left(\frac{.125}{2.7} - \frac{.125}{2.3} + 2.30\right)$$

$$= .000428$$

Then the maximum variation in tape speed is:

$$\Delta = .000282 - .000428 = .000246$$

$$or \ 0.024\%$$

Part V, Drive Belt Considerations. - Since the Iso-Elastic Drive conception is dependent on the properties of a polyester belt, it is pertinent to review some details on this item. Mylar is one of the polyester films commonly used for drive belts. Mylar belts were first developed by NASA to meet a need for more reliable drive systems for satellite recorders. According to NASA Technical Note B668, Goddard Space Flight Center "Polyester Film Belts", no belt failures occurred in the extensive test program or flight phase usage with Tiros, Vanguard II or Atlas - Score. Seamless Mylar belts are now used in most high performance space and ground instrumentation recorders. They are particularly valuable under conditions of shock and vibration because of their high strength/weight ratio. Mylar belts exhibit the following properties:

Tensile Strength:	22,000 psi
Yield Point (heat treated):	15,000 psi
Tensile Modulus (heat treated):	750,000 psi
Service Temperature:	-60^6C to $+120^oC$
Thickness Tolerance:	0.0001"
Length Tolerance:	0.010"

Simple belt tensions do not fully define belt performance. Belt life requires consideration of the complex strain distribution along the belt, including such elements as initial tension, tension in the tight and slack sides due to driving torques, and bending stress on the belt as it curves over a pulley. Initial tension is a function of the torque to be transmitted. It is given by the following equation:

$$T_o = \frac{M}{d} \ \frac{(e^{\mu\theta} + 1)}{(e^{\mu\theta} - 1)} \ .$$

50

Where

T_o = Initial Tension $\qquad$ μ = coefficient of friction

M = Torque to be transmitted $\qquad$ θ = angle of wrap

d = Diameter of the driver, $\qquad$ e = base of natural log

Stress due to the initial tension is given by:

$$S_o = \frac{T_o}{tw}$$

t = belt thickness

w = belt width

The change in stress due to transmitted torque

$$S_T = \frac{M}{dtw}$$

The bending stress can be shown as

$$\frac{Et}{d}$$

Where E is the tensile modulus.

Belt life tests have correlated actual belt life with maximum combined stress calculated in accordance with the above equations. Initial stresses below 5500 lbs. result in a belt life in excess of 50 million belt cycles. Belt requirements in the Iso-Elastic Design have been calculated in accordance with this test data, and consequently are very conservative from the standpoint of both required torque transmission and belt life.

Part VI, Discussion of System Including Magnetic Heads. - The introduction of magnetic heads into the tape path serves to complicate the analysis, and additional assumptions must be made to solve the system analytically. If we make no assumptions with regard to belt and tape speeds, the system contains eighteen (18) non-linear equations with eighteen (18) unknown quantities. This set of equations requires a computer solution.

If a specific decrease in tension across the heads is assumed, the system can be resolved to yield tape speed and tension as complicated non-linear functions of the differential, and the tape and belt properties. Tape speed is sensitive to differential only to the order of 0.1%.

An example of the tape tension profile is given below, taken from actual measurements on a 1" tape machine with 0.35% differential at 30 ips.

Location	Tension
Supply reel	20 oz.
Free span, before first of 4 heads	16 oz.
Free span, just before take-up reel	20 oz.

It is important to note that this tape tension is independent of tape direction or amount of tape already transferred.

51

APPENDIX B

ETM TAPE GUIDE ROLLER LIFE
USING REED P/N SC-0816-2Z PAIR OR EQUIVALENT

Radial load 5 oz x 0.81 = 4.0 oz.

Thrust load at 1.5 lbs. preload = 1.5 lbs.

Reed SG0816 2Z eight 1.0 mm balls

$C_{dyn} = 33$

Outer ring rotation $T/nd^2 = \dfrac{1.5}{8(0.0394)^2} = 121$. $\hspace{2cm}$ (1)

From MPB Catalog $1/2 = 3.0$

$Re = 1 \times 1.2 \times \dfrac{4}{16} + 0.712 \times 3.0 \times 1.5 = 0.3 + 3.2 = 3.5$ lbs. $\hspace{1cm}$ (2)

$Re = 0.75 \times 1.2 \times 0.25 + 3.0 \times 1.5 = 0.2 + 4.5 = 4.7$ lbs. $\hspace{1cm}$ (3)

$B_{10} = \dfrac{16667}{245} \left\{ \dfrac{53.5}{4.7} \right\}^3 = 101,000$ hours $\hspace{2cm}$ (4)

Life for P = 99.8

$Ps = e^{-\left\{ \dfrac{t}{5.35 \times 1.0 \times 10^5} \right\}^{1.34}}$ $\hspace{4cm}$ (5)

At $t = 5000$

$Ps = e^{-\left\{ \dfrac{5 \times 10^3 \times 10^{-5}}{5.35 \times 1.01} \right\}^{1.34}} = e^{-(0.925 \times 10^{-2})^{1.34}}$ $\hspace{1cm}$ (6)

$\hspace{1cm}$ 0.996 −3 = −2.034 $\longrightarrow$ −2.72 $\ = \ $ 0.28 −3 = 1.905×10^{-3} $\hspace{1cm}$ (7)

$Ps = e^{-0.00019} \cong 1 - 0.0019 = 99.8$ $\hspace{3cm}$ (8)

APPENDIX C

ESTIMATE FOR ETM FOR A 90% PROBABILITY OF SURVIVAL AT A 50% CONFIDENCE LEVEL

This estimate is based on the predicted life of the bearings and the belts that are being considered for this design. The reliability of the unit is considered to be a case of series reliability where the overall reliability is calculated as a product of the respective parts. This is given by $P_{SY} = P_1 P_2 P_3 \ldots \ldots P_m$. The exponential failure law is used to predict the probability of survival of a part as a function of time. This is derived from the Poisson distribution and is given by $P_S = E^{-\gamma'T}$. In terms of mean time between failures instead of failure rate (γ') this becomes $P_S = E^{-T}/m$ where:

P_S = probability of survival of a part

T = time in hours

E = base of the Naperian logarithim

m = mean time between failure

The method for calculating bearing life was to use the life formula where $L_{90} = \left[\dfrac{C}{R}\right]^3$ and where L_{90} is the 90% probability of survival at the 50% confidence limit. Life in millions of revolutions under the constant bearing radial load is defined as R. The basic dynamic load rating is C.

The basic dynamic load rating is based on standards established by the Anti-Friction Bearing Manufacturers Association. These standards

having been evolved from extensive design data and life test results.

Bearing life is defined as the number of revolutions which the bearing

runs before the first evidence of fatigue develops. Fatigue, in turn,

is a function of bearing load and speed. Assuming that clean, well

lubricated bearings are used other factors such as contamination and

high temperature affect the life of the bearing.

For the purposes of this estimate, a typical dynamic load rating, (c)

of 100, was selected. This value roughly represents the minimum

value, for the upper 20% of the ratings, given by New Hampshire Ball

Bearing Company. A typical bearing load, (R), of 3 lbs. was selected.

The assumption is that 1 lb. is a result of belt tension and 2 lbs. is a

result of preloading of the bearing.

To substitute the bearing life into the exponential failure function, the

bearing life must be converted into the mean time failure (m). A

convension factor of five is used to attain m. This factor is recommended

by the Barden Bearing Company.

Upon substitution into the exponential failure function the probability

of survival is then determined.

The Mylar belts were calculated, based on transmitting 0.15 oz-in. of

torque at the motor, and 0.6 oz-in. at the second and third stages of

reduction. The probability P_{be}, of survival on belts is determined by

deriving the median time to failure at the 50% confidence limit and the

life ratio is defined as Life/Median life.

54

The reliability of the system is then given by .

$$P_{SY}' = P_B \times P_{be} = 0.9703 \times 0.72 = 0.70$$

The tabulated values of belts and bearings are as follows:

PROBABILITY OF SURVIVAL OF BELTS AT 4400 HOURS

Belt	Life in Hours 95% Confidence	Life in Hours 50% Confidence	Life Ratio	π
Iso Elastic	50, 111	160, 000	0.0275	0.97
1st Stage	> 2, 880	> 9, 000	0.49	0.90
2nd Stage	11, 500	36, 000	0.12	0.90
3rd Stage	45, 000	140, 000	0.031	0.96
Interconnecting	> 40, 000	> 125, 000	0.035	0.96
			P_{be} =	0.72

π = probability of survival of an individual belt

P_{be} = product of all the individual belt probabilities

55

PROBABILITY OF SURVIVAL OF BEARINGS AT 4400 HOURS

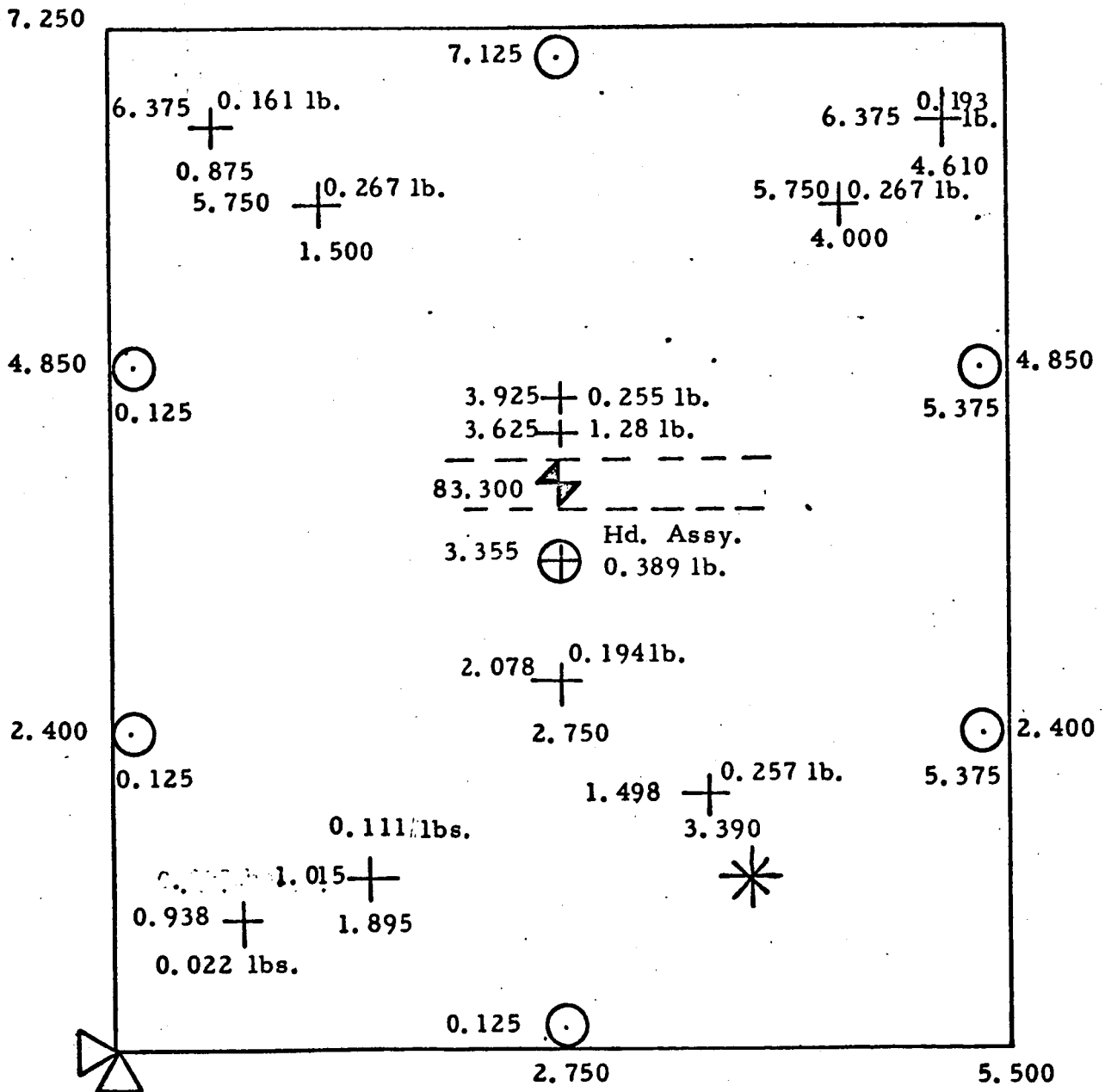| Assembly	QUA	RPM	RPH	C_{Rating}	B_{10} Life Cycles	Life Hours B10	Life Hours B50	P_{B1}
Capstan F	2	68	4,150	100	3.2×10^{10}	7.8×10^{6}	3.9×10^{7}	0.9999
Capstan S	2	68	4,150	100	3.2×10^{10}	7.8×10^{6}	3.9×10^{7}	0.9999
Motor	2	6000	360,000	100	3.2×10^{10}	8.9×10^{6}	4.5×10^{5}	0.990
First Stage	2	1350	81,000	100	3.2×10^{10}	3.6×10^{5}	1.8×10^{6}	0.9975
Second Stage	2	300	18,000	1000	3.2×10^{10}	1.8×10^{6}	9.0×10^{6}	0.9995
Idler 1	2	68	4,150	100	3.2×10^{10}	7.8×10^{6}	3.9×10^{7}	0.9999
Idler 2	2	68	4,150	100	3.2×10^{10}	7.8×10^{6}	3.9×10^{7}	0.999
Tape Pack	4	30	1,800	100	3.2×10^{10}	1.8×10^{7}	9.0×10^{7}	0.9995
Tape Guides	4	180	10,800	100	3.2×10^{10}	3.0×10^{6}	1.5×10^{7}	0.9997
							$P_B =$	0.9703

P_{B1} = probability of individual bearing survival

P_B = product of all individual bearing probabilities

B_{10} = life at 90% probability of survival

B_{50} = life at the 50% probability of survival (m)

APPENDIX D

AN ANALYSIS OF TAPE DECK LOADING

7.250

7.125 ⊙

6.375 ┼ 0.161 lb.

6.375 ┼ 0.193 lb.

0.875

5.750 ┼ 0.267 lb.

4.610

5.750 ┼ 0.267 lb.

1.500

4.000

4.850 ⊙

0.125

3.925 ┼ 0.255 lb.

3.625 ┼ 1.28 lb.

83.300

⊙ 4.850

5.375

3.355 ⊕ Hd. Assy.
0.389 lb.

2.078 ┼ 0.194 lb.

2.750

2.400 ⊙

0.125

1.498 ┼ 0.257 lb.

3.390

⊙ 2.400

5.375

0.111 lbs.

1.015 ┼

0.938 ┼ 1.895

0.022 lbs.

0.125 ⊙

2.750

5.500

Base Plate 5.500 x 7.250 x $\frac{4.61}{144}$ = 1.28 lb.

NOTE: Loading diagram assumes each load at its center of gravity.

The base plate is considered to be a solid plate except for the wire throughs.

57

APPENDIX D (Continued)

CENTER OF GRAVITY OF LOADS

x	p	xp	y	yp
0.650	0.022	0.0143	0.938	0.0206
1.895	0.111	0.2100	1.015	0.1128
3.390	0.257	0.8720	1.438	0.3695
2.750	0.195	0.5360	2.078	0.4050
2.750	0.389	1.0700	3.355	1.3030
2.750	1.280	3.5200	3.625	4.6450
2.750	0.255	0.7015	3.925	1.0010
0.875	0.161	0.1410	6.375	1.0280
1.500	0.267	0.4005	5.750	1.5380
4.000	0.267	1.0690	5.750	1.5380
4.610	0.193	0.8900	6.375	1.2300
	3.377	8.4243		13.1909

$$\bar{x} = 2.495 \text{ inches} \qquad \bar{y} = 3.900 \text{ inches}$$
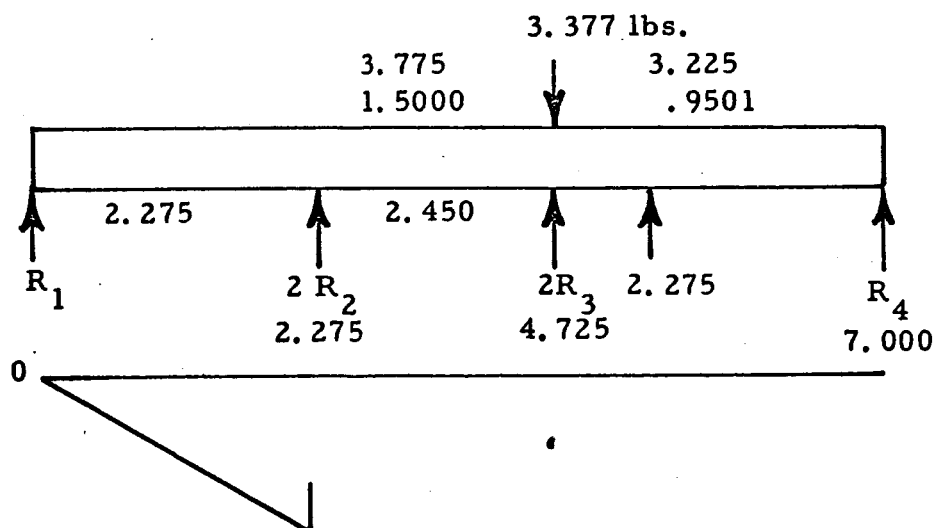
APPENDIX D (Continued)

Using three moment equations: $M_1 = M_4 = 0$ (1)

$$M_1 \, 2.275 + 2M_2 \, 4.725 + M_3 \, 2.450 = \frac{-3.377 \times 0.750}{2.450} \, (2.450 - 95^{-2}) \quad (2)$$

$$9.450M_2 + 2.450M_3 = 1 - 1.032 \, (6.0025 - 0.9025) \quad (3)$$
$$= -1.032 \times 5.10 = -5.27$$

$$M_4 \, 2.275 + 2M_3 \, 4.725 + M_2 \, 2.450 = \frac{-3.377 \times 1.500}{2.450} \, (2.450^{-2} - 1.50^{-2}) \quad (4)$$

$$2.450M_3 + 2.450M_2 = -2.064 \, (6.0025 - 2.25)$$
$$= -2.064 \, (3.7525) = -7.75 \quad (5)$$

$$9.450 \, M_2 + 2.450 \, M_3 = -5.27$$

$$9.450 \, M_2 + 36.41 \, M_3 = -29.85$$

$$33.96 \, M_3 = -24.58$$

$$M_3 = -0.724 \text{ lb. in.} \quad (6)$$

$$9.45 \, M_2 \times 2.45 \times -0.724 = -5.27 \quad (7)$$

$$9.45 \, M_2 = -5.27 + 1.77 = -3.50 \quad (8)$$

$$M_2 = -0.370 \text{ lb. in.} \quad (9)$$

but $M_2 = 2.275 \, R_1 = -0.370$ (10)

$$R_1 = -0.163 \text{ lb.} \quad (11)$$

$$M_3 = 2.275 \, R_4 = -0.729 \quad (12)$$

$$R_4 = -0.318 \text{ lb.} \quad (13)$$

APPENDIX D (Continued)

$M_3 = 0$ $4.90 R_2 = 4.725 \times 0.163 + 3.377 \times 0.950 - 2.275 \times 0.318$ (14)
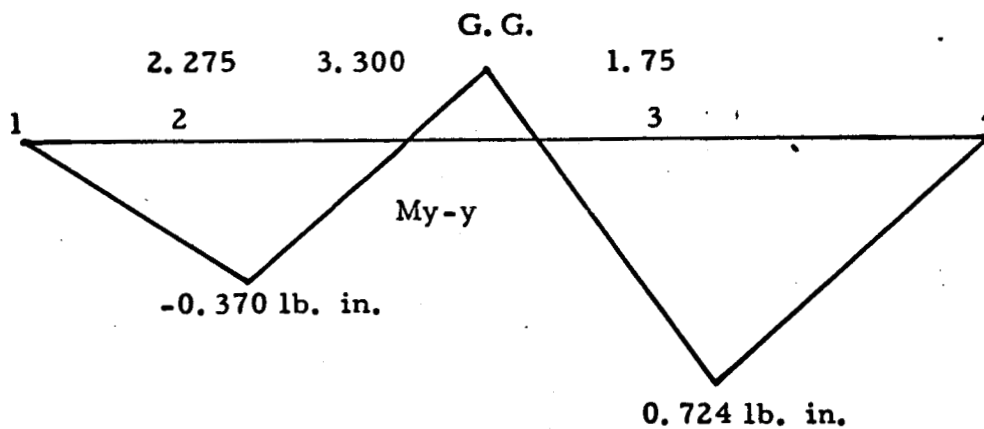
$= 0.770 + 3.205 - 0.729$

$= 3.251$

$R_2 = 0.664$ lb.   (15)

$M_2 = 0$ $4.90 R_3 = 1.500 \times 3.377 + 4.725 \times 0.318 - 2.275 \times 0.163$ (16)

$= 5.06 + 1.501 - 0.371$

$= 6.19$

$R_3 = 1.26$ lbs.   (17)

Moment Diagram

$M_{y-y} = -0.370 + 1.165 \times (3.300 - 2.275)$

$= -0.370 + 1.165 \times 1.025$

$= 0.370 + 1.195$

$= 0.825$ lbs. in/g

$m_{x-x} = 0$ since load centered on end support

APPENDIX D (Continued)

Stress per g acceleration

$$S_{solid} = \frac{Mc}{F} = \frac{0.825 \times 6}{0.5^{-2}} = 19.8 \text{ psi/g} \tag{14}$$

$$S_{grooved} = \frac{0.825 \times 6}{0.312^{-2}} = 50.9 \text{ psi/g} \tag{15}$$

At 15 g acceleration

$$S_{solid} = 297 \text{ psi} \tag{16}$$

$$S_{grooved} = 763 \text{ psi} \tag{17}$$

61

APPENDIX E

REPORT ON ELECTRON-BEAM
WELDING METHODS FOR ETM HOUSING
AT NORTH AMERICAN AVIATION

Welding in a heavy inert gas atmosphere by the tungsten resistance method is not a true Electron-Beam process. In this process a tungsten rod is traced along the welding seam of the grounded housing creating a arc welded seam of a more precise nature than that usually associated with this process. Two main drawbacks to this approach as opposed to Electron-Beam welding are, high heat generation, and a moderately wide seam.

If the Electron-Beam is used, the Recorder will be subjected to maximum vacuum of 10^{-4} for a maximum time of 4 hours. This time is based on an estimate as to how long it will take to weld the four sides of the housing. If desired, the chamber can be returned to atmospheric pressure after each welding pass. This cycling will increase the overall processing time.

Welding of the headers and pressurizing valve to the housing by the Electron-Beam method presents some problems due to the dissimilarity of the metals, covar to aluminum, and stainless steel to aluminum. This condition can probably be overcome by a form of electron-beam brazing.

Heat penetration into the deck is not expected to be high due to the wide dimension on the joining lip of the housing. This lip is 0.250 inches wide and the expected beam would be from 0.060 to 0.125 inches deep ± 0.010.

APPENDIX E (Continued)

The required depth will be determined from preliminary pressure tests.
Once a seam width is selected, heat penetration into the deck will be
checked by including a dummy deck which would be painted with temperature
sensitive chemicals.

Due to the relative uncertainty of the preceding approaches, North American
Aviation feels it necessary to do preliminary test work to assure the
optimum use of the various processes available at their facility. Once
established, this ground work would not have to be retraced for this or
similar housings of comparable design. The estimated cost up to and including
the welding of the first two test housings is approximately $700.00 This
amount would be deposited into an account with the understanding that any
surplus would be used at a later date, with as little as one day notice, for
future housing welding. Estimated time for processing one housing, after
testing, is one day. Kinelogic during the preliminary phase is to insure
compatability and would upon completion of a finished housing furnish
certification of housing seal validity.

Other points discussed were:

   1) Selection of housing material from a welding standpoint.

      a) In the following order, titanium and magnesium
         are more desireable than aluminum.

      b) Of the aluminum alloys, the 6000 series is the
         least desireable. The 5000 series is the better
         alloy.

63

APPENDIX E (Continued)

Another application for Electron-Beam welding is the welding of the multipin headers to the case. Electron-Beam welding has been used to produce hermetically sealed joints and without distrubing the glass to metal seal at the pins in reactive materials no definite leakage rate could be attained. It would be expected that leakage rates equivalent to the base material would have a lower leakage rate than an elestomer type seal.

It is acknowledged that a present, the technology and facilities for Electron-Beam welding is sufficient to produce hermetic joints on the ETM housing and the same process can also be used for welding in the multipin headers. The main limitation of the process is the time required to open up a joint which is more time than required to open up a Gasko Seal. Servicing of the recorder, after the housings have been welded would be delayed, pending the opening of the Electron-Beam welded joints.

Whether Gasko Sealed covers or the Electron-Beam welded covers are used, it was felt that the structural integrity of the covers in a hard vacuum environment required analysis. As shown below, the maximum stress and deflection are due to atmosphereic differential pressure and is calculated for both aluminum and magnesium alloys.

64

APPENDIX E (Continued)

Stress and deflection on cover of ETM

p = 15 psi (1 at differential)

Type loading = Uniform

Type support = All edges fixed

Total load F = abp.

$$F = 6 \text{ in.} \times 7.75 \text{ in.} \times 15 \text{ psi} = 700 \text{ lbs.}$$

Maximum stress = $S_b = \dfrac{0.5 \, b^2 p}{t^2 \left(1 + 0.623 \dfrac{b^6}{a^6}\right)}$ (1)

$$S_b = \frac{0.5 \times 6^2 \times 15}{0.125^2 \left\{1 + 0.623 \left\{\dfrac{6^6}{7.5^6}\right\}\right\}}$$ (2)

$$= \frac{270}{0.0156 \left(1 + 0.623 \left\{\dfrac{46560}{216380}\right\}\right)}$$

$$= \frac{270}{0.0156 \left(1 + 0.134\right)}$$

$$= \frac{270}{0.0156 \left(1.134\right)} = \frac{270}{0.0177} = 15300 \text{ psi}$$ (3)

For aluminum alloy 6061T6, Sy = 40000 psi

This gives a margin of safety of 1.6.

For AZ31B-H24 magnesium, Sy = 24000 psi

This gives a margin of safety of 0.5%

65

APPENDIX E (Continued)

$$\underline{\text{Maximum deflection}} \ y \ max = \frac{0.0284 \ b^5 p}{Et^3 \left\{ 1 + 1.056 \ \dfrac{b^5}{a^5} \right\}}$$

$E = 10 \times 10^6 = $ aluminum

$E = 6.5 \times 10^6 = $ magnesium

$$\begin{aligned} y \ max \\ \text{(aluminum)} \end{aligned} = \frac{0.0284 \ (1296 \times 15)}{10 \times 10^6 \times .125^3 \ (1 + 1.056) \left\{ \dfrac{7776}{27923} \right\}} \qquad (1)$$

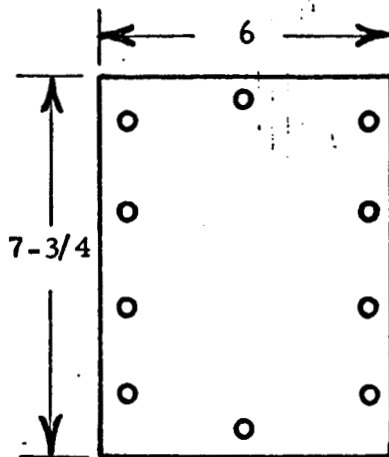$$= \frac{550}{10 \times 10^6 \times 1.95 \times 10^{-3} \ (1.295)}$$

$$= \frac{550}{10^4 \times 5.75} = 96.0 \times 10^{-4} = 0.0096 \qquad (2)$$

$$y \ max. \ (mag) = \frac{10}{6.5} \times 0.0096 = \underline{0.014} \qquad (3)$$

APPENDIX E (Continued)

When considering the Gasko Seal method of sealing, an analysis of the cover bolts was made. This analysis given below indicates a maximum safety margin of 2.76.
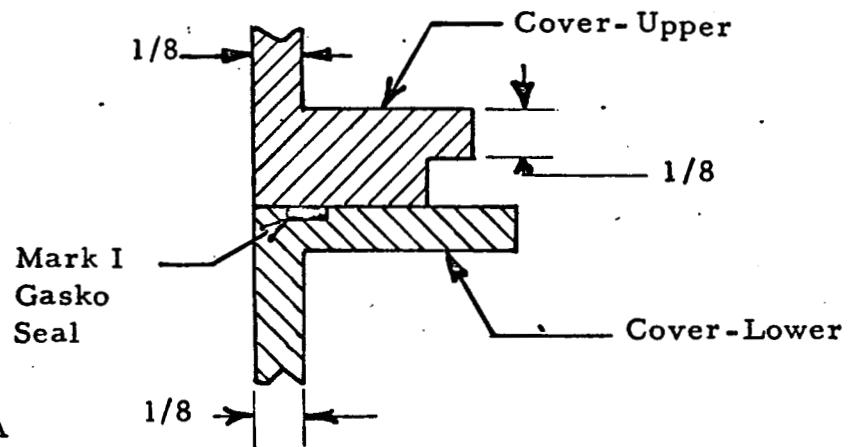
CALCULATION ON BOLT STRESS - ETM COVER

Bolts are 8-32 machine bolts

Effective stress area

$A_e = .0139 \text{ in}^2$

N = Number of bolts (10

Cover-Upper

Mark I Gasko Seal

Cover-Lower

Projected area of cover = A

$A = 5.75 \times 7.5 = 43 \text{ in}^2$

15 psi

$P = 15 \text{ psi} \times 43 \text{ in}^2 = 645 \text{ lbs.}$ where p = force due to pressure

The recommended bolt force for a Mark I seal equals 25 lbs. per linear inch of seal. With an approximate seal length of 26 inches, the minimum required bolt force = 26 in x 25 lbs in = 650 lbs. Therefore the minimum-installed-bolt-force would have to be 650 lbs + 645 lbs. or 1295 lbs. The minimum stress per bolt becomes: $S \text{ min} = \dfrac{P}{N \times Ae} = \dfrac{1295}{10 \times .0139} = 9,300 \text{ psi.}$

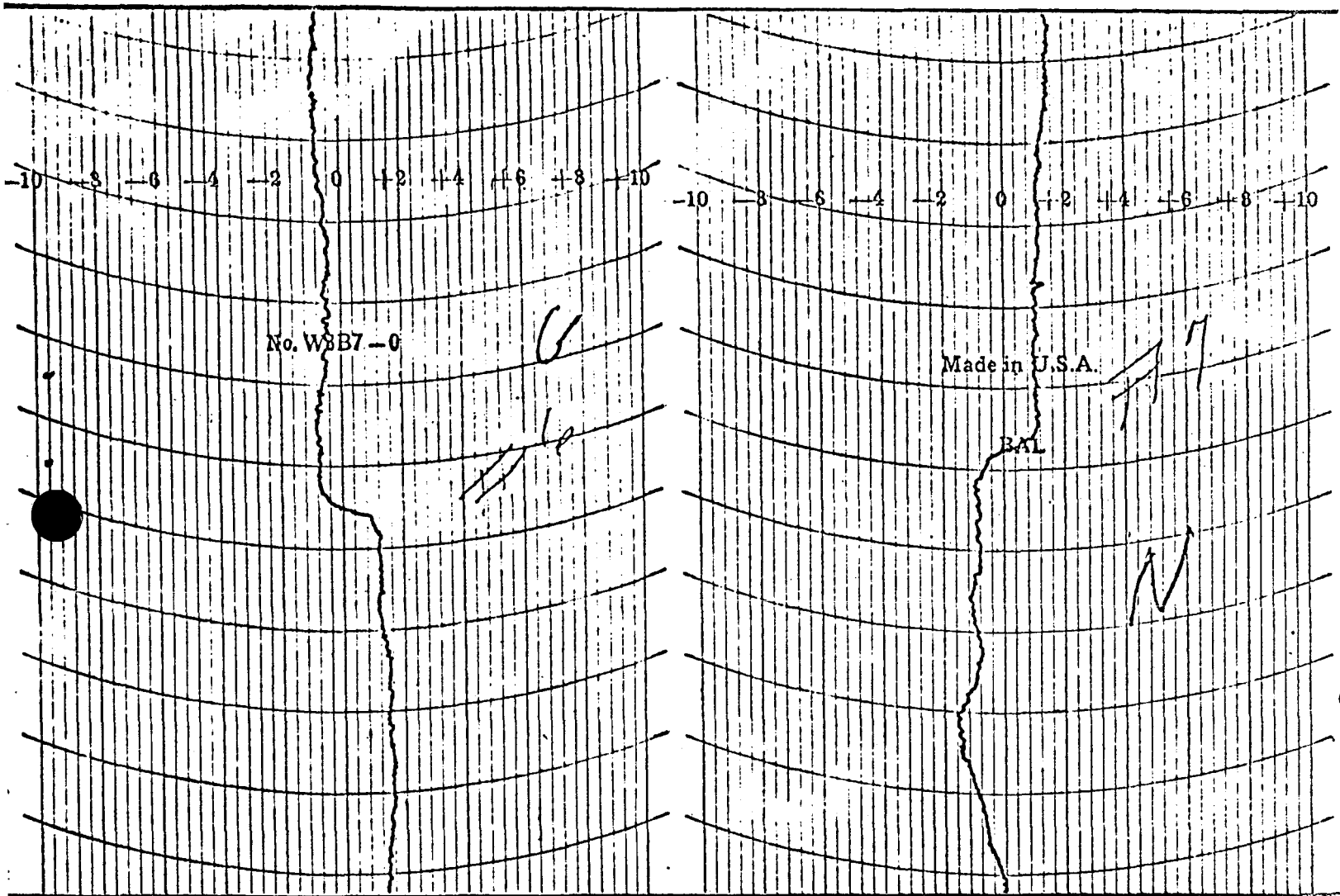The margin of safety using S_y equals 35,000 psi for 303 ST. STL is

$\dfrac{35000 \text{ psi} - 9300 \text{ psi}}{9300} = 2.76 \text{ psi}$
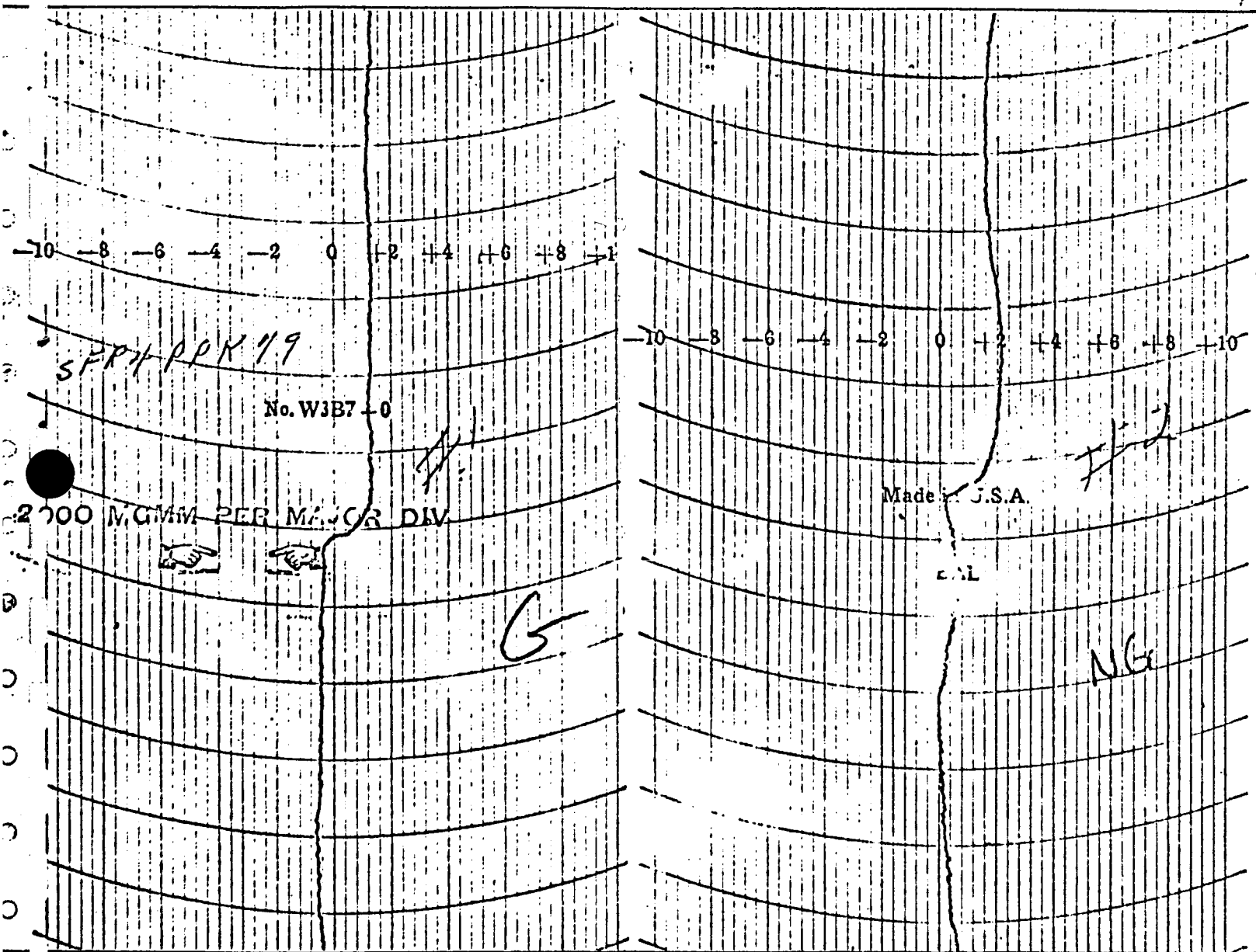
67

APPENDIX F

BEARING TORQUE TRACES

TYPICAL TORQUE TRACES FOR BEARINGS USED IN THE
TENSION ARM ASSEMBLY, 1st STAGE, 2nd STAGE, SLOW
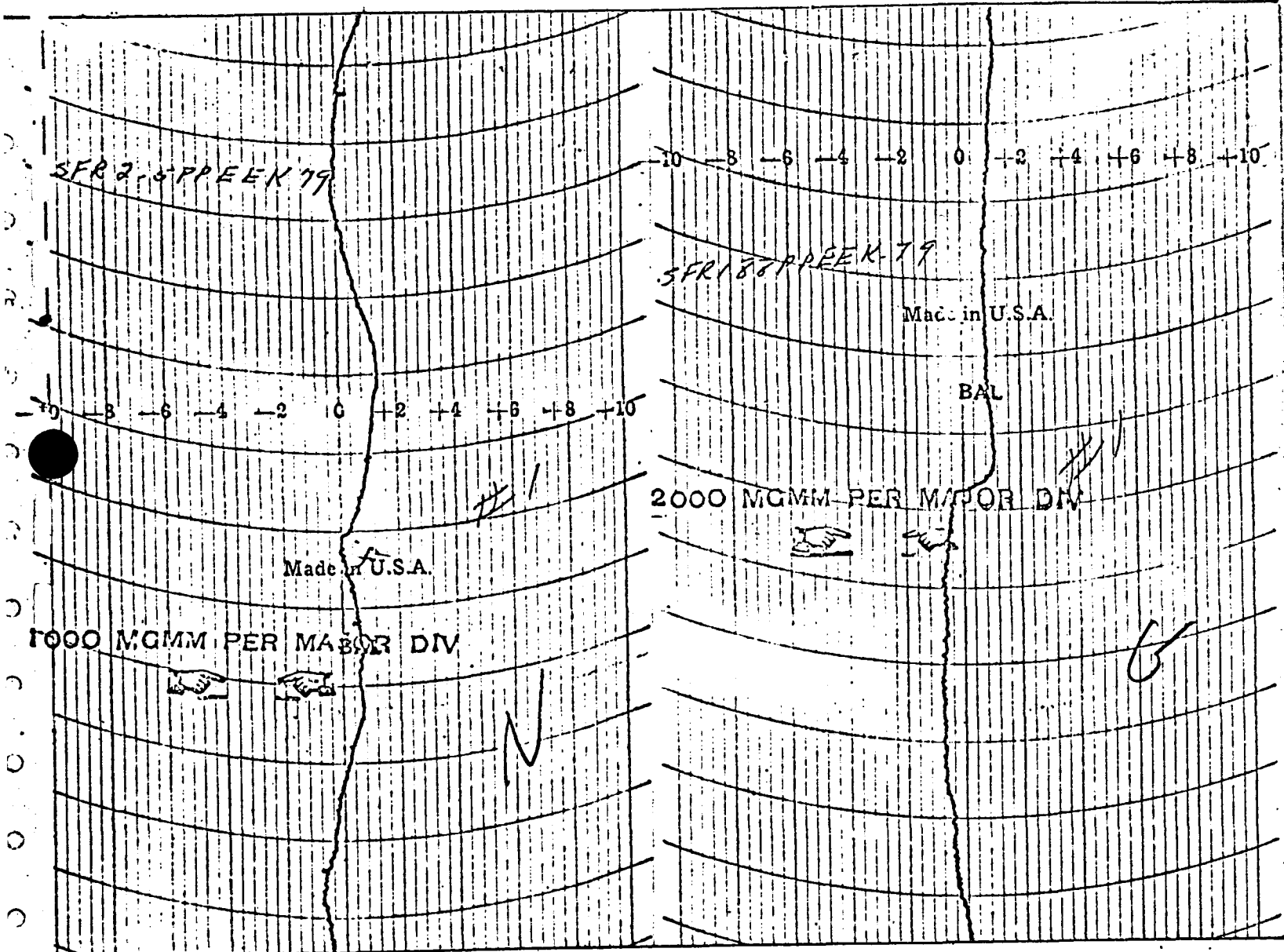CAPSTAN, FAST CAPSTAN and ISO-BELT IDLER.

APPENDIX F

BEARING TORQUE TRACES

TYPICAL TORQUE TRACES FOR BEARINGS USED IN REEL HUB ASSEMBLIES

APPENDIX F

BEARING TORQUE TRACES

TYPICAL TORQUE TRACES FOR
BEARINGS USED IN THE TAPE
GUIDE ROLLER ASSEMBLY.

TYPICAL TORQUE TRACES FOR
BEARINGS USED IN THE IDLER
ASSEMBLY PIVOT.

APPENDIX G

BEARING CHARACTERISTICS

GENERAL DESCRIPTION for 3/16 x 1.2 inch flanged bearing.

Manufacturer's Basic Designation: New Hampshire B-B: SFR3PP

Reed B-B: SP 1232 2Z.

Basic Dimensions: Bore 0.18750 /0.18730 inches.

O. D. 0.5000/0.49980 inches.

Width: 0.196/0.195 inches.

Dimensional Tolerances: ABEC-7P.

Material: Vacuum melt AISI 400 C Stainless Steel.

Shield or seal: Seal on flanged end. Shield on unflanged end.

Retainer: Phenolic.

Radial Play or Contact angle: 0.0007/0.0009 inch radial play.

Lubrication: Lubricant: Bendix P-10 filtered 1.2 micron maximum.

Application: 2-4 milligram metered into ball.

Configuration: Single area. Vacuum impregnate retainer and centrifuge

retained at 25 G's for 1 minute.

Preload: None.

Torque, Starting: 5000 mg-mm average with a 75 gm test load.

Torque, Running: 2500 mg-mm average with a 75 gm test load.

Other: Supply following documentation:

1.   Tabulation of 10 starting torque measures (w/o seal).

2.   Running torque trace per Mil Std. 206A.
Maximum hash width not to exceed 5000 mg-mm (w/o seal).

3.   Tallyrond or Indi-ron traces on bore and bore track of inner
and outer ring. Roudness limit equals 50 micro-inches.

71

APPENDIX G (Continued)

GENERAL DESCRIPTION for 1/8 x 5/16 inch flanged bearing extended inner ring.

Manufacturer's Basic Designation: New Hampshire B-B: SFR 2-5PPEE

Reed B-B: SH 0820 2Z.

Basic Dimensions: Bore 0.1250/0.1248 inch.

O.D. 0.3125/0.3123 inch.

Width: 0.1406/0.1396 inch outer ring.

0.1718/0.1708 inch inner ring.

Dimensional Tolerances:

Material: Vacuum melt AISI 440 e Stainless Steel.

Shield or seal: Seal on flanged end. Shield on unflanged end.

Retainer: Phenolic.

Radial Play or Contact angle: 0.0007/0.0009 inch radial play.

Lubrication: Lubricant: Bendix B-10 filtered 1.2 micron maximum.

Application: 1/2 - 1 milligram metered into ball area.

Impreganted retainer and centrifuge.

Retainer at 25 G's for - minute.

Configuration: Single.

Preload: None.

Torque, Starting: 900 mg-mm average with a 75 gm test load.

Torque, Running: 800 mg-mm average with a 75 gm test load.

Other: Supply the following documentation:

1. Tabulation of 12 starting torque traces (w/o seal).

2. Running torque trace per Mil Std. 206A.

   Maximum task width not to exceed 1500 mg-mm (w/o seal).

3. Tallyrond or Indi-Ron traces on bore and bore track of inner
   and outer ring. Roudness limit equals 50 micro-inches.

APPENDIX G (Continued)

GENERAL DESCRIPTION: 1/4 x 1/2 Flanged Bearing

Manufacturer's Basic Designation: New Hampshire B-B: SFRI 88 PPEE

Reed B-B: SH 1632 2Z

Basic Dimensions: Bore 0.2500/0.2498 inches.

O.D. 0.5000/0.4998 inches.

Width: 0.1875/0.1865 inches outer ring.

0.2187/0.2177 inches inner ring.

Dimensional Tolerances: ABEC-7P.

Material: Vacuum melt AISI 440 C Stainless Steel.

Shield or seal: Seal on flanged end. Shield on unflanged end.

Retainer: Phenolic.

Radial Play or Contact angle: 0.0007/0.0009 inch radial play

Lubrication: Lubricant: Bendix P-10 filtered 1.2 micron maximum.

Application: 4-6 milligram metered into ball area.

Impregnate retainer and centrifuge.

Configuration: Single retainer at 25 g's for 1 minute.

Preload: None

Torque, Starting: 5000 mg-mm average with a 400 gm test load.

Torque, Running: 3500 mg-mm average with a 400 gm test load.

Other: Supply following documentation:

1. Tabulation of 10 starting torque measures (w/o seal).

2. Running torque trace per Mil Std. 206A.
   Maximum hash width not to exceed 5000 mg-mm (w/o seal).

3. Tallyrond or Indi-ron traces on bore and bore track of inner
   and outer ring. Roudness limit equals 50 micro-inches.

APPENDIX G (Continued)

GENERAL DESCRIPTION: 1/4 x 5/8 inch flanged bearing

Manufacturer's Basic Designation: New Hampshire B-B: SFR4PP

Reed B-B: SP 16402Z.

Basic Dimensions: Bore 0.2500/0.2498 inches.

O.D. 0.6250/0.6248 inches. .

Width: 0.196/0.195 inches.

Dimensional Tolerances: ABEC-7P.

Material: Vacuum melt AISI 400 C Stainless Steel.

Shield or seal: Seal on flanged end. Shield on unflanged end.

Retainer: Phenolic.

Radial Play or Contact angle: 0.0007/0.0009 Radial Play.

Lubrication: Lubricant: Bendix P-10 filtered 1.2 micron maximum.

Application: 4-6 milligram metered into ball area.

Impregnate retainer and centrifuge.

Configuration: Single retainer at 25 g's for 1 minute.

Preload: None.

Torque, Starting: 4000 mg-mm average with a 400 gm test load.

Torque, Running: 4000 mg-mm average with a 400 gm test load.

Other: Supply following documentation:

1. Tabulation of 10 starting torque measures (w/o seal).

2. Running torque trace per Mil Std. 206A.

Maximum hash width not to exceed 6000 mg-mm (w/o seal).

3. Tallyrond or Indi-ron traces on bore and bore track of inner

and outer ring. Roudness limit equals 50 micro-inches.

74